Joint Allocation Strategies of Power and Spreading Factors With Imperfect Orthogonality in LoRa Networks

Licia Amichi, Megumi Kaneko, *Senior Member, IEEE*, Ellen Hidemi Fukuda, Nancy El Rachkidy, and Alexandre Guitton

Abstract—The LoRa physical layer is one of the most promising Low Power Wide-Area Network (LPWAN) technologies for future Internet of Things (IoT) applications. It provides a flexible adaptation of coverage and data rate by allocating different Spreading Factors (SFs) and transmit powers to end-devices. We focus on improving throughput fairness while reducing energy consumption. Whereas most existing methods assume perfect SF orthogonality and ignore the harmful effects of inter-SF interferences, we formulate a joint SF and power allocation problem to maximize the minimum uplink throughput of end-devices, subject to co-SF and inter-SF interferences and power constraints. This results into a mixed-integer non-linear optimization, which, for tractability, is split into two sub-problems: firstly, the SF assignment for fixed transmit powers, and secondly, the power allocation given the previously obtained assignment solution. For the first sub-problem, we propose a low-complexity many-to-one matching algorithm between SFs and end-devices. For the second one, given its intractability, we transform it using two types of constraints' approximation: a linearized and a quadratic version. Our performance evaluation demonstrates that the proposed SF allocation and power optimization methods enable to drastically enhance various performance objectives such as throughput, fairness and power consumption, and that they outperform baseline schemes.

Index Terms—LoRa, spreading factor, resource allocation optimization, matching theory.

I. Introduction

A WIDE range of applications will be enabled by the advent of Internet of Things (IoT) technology, among which smart cities, intelligent transportation systems and environmental monitoring. Given the expected proliferation of such IoT devices in the near future, providing tailored wireless communication protocols with high spectral efficiency and low power consumption is becoming ever more urgent. Indeed, many of these services will depend on IoT Wireless Sensor Networks (WSNs), supported by newly developed Low-Power Wide-Area Network (LPWAN) technologies such as LoRa, SigFox or Ingenu [2]–[5]. LPWANs are generally single-hop wireless networks, where end-devices are connected wirelessly to gateways, and gateways are interconnected through Internet to a network server, forming a star-of-stars topology.

The LoRa physical layer uses the Chirp Spread Spectrum (CSS) modulation technique, where each chirp encodes 2^m values. Parameter m is referred to as the Spreading Factor (SF) as defined in [6], and multiple end-devices may use the same channel simultaneously through different SFs. One of the most popular LPWAN technology based on the LoRa physical layer is the LoRaWAN standard of LoRa Alliance [7], which defines the MAC layer protocol based on ALOHA mechanism [4]. It is an increasingly used LPWAN technology, as it operates in the ISM unlicensed bands and enables a flexible adaptation of transmission rates and coverages under low energy consumption [6]. Namely, smaller SFs provide higher data rates but reduced ranges, while larger SFs allow longer ranges but lower rates [5].

The main issue of LoRa-based networks such as LoRaWAN is their inherent throughput limitation: the physical bitrate varies between 300 and 50000 bps [7]. Besides, collisions are very harmful to the system performance as the gateway is unable to correctly decode simultaneous signals sent by devices using the same SF on the same channel. Such interferences will be referred to as co-SF interferences. Although SFs were widely considered to be orthogonal among themselves, some recent studies have demonstrated through real-world experiments [8]–[10] that this was not the case, namely that signals using different SFs on the same channel may interfere among themselves, hereafter referred to as inter-SF interferences [11].

In order to improve the LoRa system performance, a number of works have proposed resource optimization methods [12]–[14]. These works have tackled the issues of channel, spreading factor, or transmit power allocation and optimization. However, most papers, so far, have assumed perfect orthogonality among SFs and hence are not adapted to the real-world conditions where the effects of imperfect SF orthogonality cannot be ignored.

Therefore, in this work, we investigate the issues of SF and transmit power allocation optimization under both co-SF and inter-SF interferences, for a LoRa network that would use a generic slotted MAC protocol enabling scheduling of the end-devices. Unlike our preliminary work [1] which only considered SF allocation under fixed transmit power, and treated the cases of co-SF and inter-SF interferences separately, we now tackle both the SF and power allocation under a generalized co-SF and inter-SF interference modeling. The goal of this work is to provide insights on the theoretically achievable MAC layer performance in order to serve as a benchmark for any practical MAC layer, depending on which specific overheads and losses would occur. We focus on the problem of maximizing the minimum achievable short-term average rate in the uplink, whereby short-term average rate is defined as the average rate over random channel fading, but given a fixed position of end-devices. This metric is especially suited for LoRa networks, since the end-devices will likely be fixed for a certain period of time (at least for a few seconds) in many applications, and their positions known at the gateway, as in conventional signal-strength-based SF allocation methods [7]. Firstly, we formulate a joint SF assignment and power allocation problem by modeling the achievable uplink short-term average rate under co-SF and inter-SF interferences, and power constraints. Next, given the mathematical intractability of this mixed-integer optimization problem, we split it into two sub-problems: SF assignment under fixed transmit power, then transmit power allocation given the previous SF assignment solution. To solve the first sub-problem, we propose an SF-allocation algorithm based on matching theory. We show its stability and convergence properties, and analyze its computational complexity. Next, we transform the second sub-problem into an equivalent feasibility problem with non-linear constraints. To make it tractable, we propose to approximate the constraints in two different ways: linear and quadratic. The numerical results show that, compared to baseline schemes, our proposed method not only provides larger minimum rates, but also jointly improves the network throughput and fairness level. Moreover, the proposed power control further improves the performance in terms of minimum rates and user fairness, while realizing massive power savings.

The remainder of this paper is organized as follows. Section II presents the related works. Section III describes the system model. Section IV presents our joint SF and transmit power allocation problem and its constraints. Section V details a low-complexity many-to-one matching algorithm for the first sub-problem. Section VI discusses our transmit power allocation scheme for the second sub-problem. Section VII studies the performance of the proposed algorithms. Finally, Section VIII presents our conclusions.

II. Related Works

Recent studies have shown through real-world experiments as well as computer simulations, the non-negligible effects of inter-SF interferences [8]–[10]. Authors in [11] analyzed the achievable uplink LoRa throughput under imperfect SF orthogonality, and have theoretically demonstrated the harmful impact of both co-SF and inter-SF interferences on the overall throughput. Reference [15] also showed the non-negligible effects of SF orthogonality. Authors in [10] also unveiled a significant drop in performance when taking into account the inter-SF interferences in high-density deployments. In [16], the authors proposed a model for analyzing the performance of a multi-cell LoRa system considering co-SF interference, inter-SF interference, and the aggregated intra and inter-cell interferences. They also highlighted the necessity for an SF allocation scheme accounting for these interferences.

Extensive studies have been carried out to enhance the LoRa system performance by proposing resource optimization methods [12], [13]. However, most papers, so far, have assumed perfect orthogonality among SFs. In particular, the authors in [12] designed a channel and power allocation algorithm that maximizes the minimal rate. However, no SF allocation nor SF-dependent rates were considered, despite the strong dependency of the rate to SFs. In addition, the solution of [12] requires instantaneous Channel State Information (CSI) feedback, which is not adapted to LoRa networks due to their energy consumption limitations [7]. In [13], a heuristic SF-allocation is proposed in addition to a transmit power control algorithm, where end-devices with similar path losses are simply assigned to the same channel with different SFs, according to their distance to the gateway. Although the issue of inter-SF interferences was highlighted, it was ignored in their proposed solution. Moreover, all end-devices are required to be able to successfully receive all SFs. The authors of [14], [17] proposed a method for decoding superposed LoRa signals using the same SF, as well as a full MAC protocol enabling collision resolution, the combination of which was shown to drastically outperform LoRaWAN jointly in terms of network throughput, delay, and energy efficiency. Finally, reference [18] extended the channel allocation method of [12] by investigating power allocation, and proposed an algorithm based on Markov decision process.

III. System Model

We consider a LoRa-based system with one network server and one gateway. The network server is a centralized entity which is in charge of controlling the data rate and the transmission power of end-devices as in, e.g., LoRaWAN through ADR (adaptive data rate) commands [7]. Thus, our algorithm can be run in the network-server. The gateway is located at the center of a circular cell of radius R km and N end-devices randomly distributed within it and simultaneously active, as depicted in Figure 1. We denote by $\mathcal{N}$ the set of end-devices and by
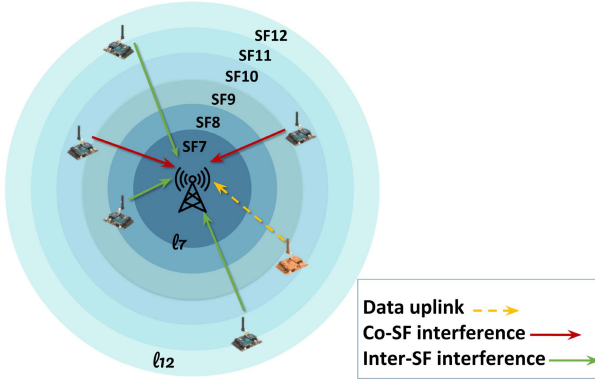
Fig. 1. LoRaWAN network, with end-devices transmitting simultaneously on various SFs.

$\mathcal{M} = \{7, 8, \ldots, 12\}$ the set of available SFs. Note that the proposed method is applicable to different sets of SFs.

A. PHY Parameters' Description

We assume that all end-devices transmit on the same channel c of bandwidth BW, with a duty cycle of $d\%$ as imposed by regulations such as ETSI for Europe. The data bit-rate R_m of SF m, $m \in \mathcal{M}$, is given by [6],

$$R_m = \frac{m \times CR}{\frac{2^m}{BW}}, \tag{1}$$

where $CR = \frac{4}{4+x}$ is the coding rate, with $x \in \{1, 2, 3, 4\}$.

Although the proposed method is not based on LoRaWAN's ALOHA protocol, we assume without loss of generality the same set of SFs as for LoRaWAN, i.e., six SFs from 7 to 12.

Let h_n be the small-scale channel fading gain between end-device n and the gateway, f_c the carrier frequency and $A(f_c) = (f_c^2 \times 10^{-2.8})^{-1}$ the deterministic path-loss term [11]. The uplink instantaneous Channel-to-Noise Ratio (CNR), ζ_n, for end-device n at SF m is given by [11],

$$\zeta_n = \frac{|h_n|^2 A(f_c)}{r_n^\alpha \sigma_c^2}, \tag{2}$$

where r_n is the distance from end-device n to the gateway, α is the path loss exponent and $\sigma_c^2 = -174 + NF + 10\log_{10}(BW)$ dBm is the Additive White Gaussian Noise (AWGN) and NF is the receiver noise figure. Hence, the path loss is given by $A(f_c)/r_n^\alpha$. Assuming Rayleigh fading channels, the CNR ζ_n is modeled as an exponential random variable with mean $\overline{\zeta}_n = \frac{A(f_c)}{r_n^\alpha \sigma_c^2}$.

The area covered by each SF is given by the distance ranges in Table I [11],

$$l_m = \left(\frac{P_{\max} A(f_c)}{q_m} \right)^{\frac{1}{\alpha}}, \tag{3}$$

given the receiver sensitivity q_m of each SF m in Table I and $P_{\max}$ the maximal transmit power. Hence, larger SFs result in larger communication ranges, with $l_{12} = R$. In proposed and reference algorithms, the distance of each end-device to the gateway is assumed to be known at the gateway, as an output of the PHY layer channel (path-loss) estimation.

TABLE I
LoRa Characteristics at $BW = 125\text{kHz}$ [11]

SF m	Bit-rate R_m [kb/s]	Receiver sensitivity q_m [6] [dBm]	Reception thresh. $\theta_{\mathrm{rx}\,m}$ [dB]	InterSF capture thresh. [8] $\hat{\theta}_m$ [dB]	Distance ranges [km]
7	5.47	-123	-6	-7.5	$[0, l_7]$
8	3.13	-126	-9	-9	$(l_7, l_8]$
9	1.76	-129	-12	-13.5	$(l_8, l_9]$
10	0.98	-132	-15	-15	$(l_9, l_{10}]$
11	0.54	-134.5	-17.5	-18	$(l_{10}, l_{11}]$
12	0.29	-137	-20	-22.5	$(l_{11}, l_{12}]$

Next, we denote the SF assignment by s_{ij} and define it as,

$$s_{ij} = \begin{cases} 1, & \text{if end-device } i \text{ uses SF } j \\ 0, & \text{otherwise.} \end{cases}$$

If there is only one end-device n assigned to SF m, this end-device is only subject to inter-SF interferences caused by end-devices using a different SF. Hence the inter-SF Signal-to-Interference-plus-Noise-Ratio (SINR) of end-device n can be expressed as,

$$\text{SINR}_{nm}^{\text{inter}} = \frac{\zeta_n p_{nm}}{\sum\limits_{i \in \mathcal{N}_{-n}} \sum\limits_{j \in \mathcal{M}_{-m}} s_{ij} p_{ij} \zeta_i + 1}, \tag{4}$$

obtained by dividing the signal power (numerator) and interference-plus-noise power (denominator) by the noise power σ_c^2. In (4), p_{nm} is the transmission power of the end-device n at SF m, $\mathcal{N}_{-n} = \mathcal{N} \setminus \{n\}$ and $\mathcal{M}_{-m} = \mathcal{M} \setminus \{m\}$.

When there is more than one end-device assigned to an SF, these devices are subject to both inter-SF and co-SF interferences. Therefore, the co-SF SINR of device n on SF m is written as,

$$\text{SINR}_{nm}^{\text{co}} = \frac{\zeta_n p_{nm}}{\sum\limits_{i \in \mathcal{N}_{-n}} \sum\limits_{j \in \mathcal{M}_{-m}} s_{ij} p_{ij} \zeta_i + \sum\limits_{i \in \mathcal{N}_{-n}} s_{im} p_{im} \zeta_i + 1}. \tag{5}$$

Note that this is a more general model as compared to that of [1], which assumed the dominance of co-SF interferences over inter-SF interferences. In conformity to LoRa standards, instantaneous CSI feedback is not assumed, unlike [12]. Hence, the SF allocation is performed every period of time, during which the long-term fading instance, i.e., path loss, can be assumed to be fixed. This is well suited to a wide range of applications envisioned for IoT systems based on LoRa, expected to be static, or with low mobility [19]. Therefore, the achievable uplink short-term average rate for end-device n at SF m is given similarly to [11] by,

$$\tau_{nm} = R_m \times P_{\text{cap}}^{(n,m)}, \tag{6}$$

where $P_{\text{cap}}^{(n,m)}$ is the probability of successful reception analyzed in the following section.

B. MAC Layer Description

The analytical throughput model above, as shown in [11], corresponds to a generic slotted MAC protocol with

perfect synchronization. With a limited overhead, it is possible to implement a MAC protocol that does not assume a perfect synchronization, as follows. Periodically, the network server generates a beacon that is broadcasted by all gateways. These beacons allow the end-devices to be synchronized, and contain the information about the number of slots for SF 12 ($n_{\text{slots},12}$), and the transmission schedule for all nodes that results from our proposed SF and power allocation optimization. The nodes' transmission schedule define for each scheduling period between two beacons, the active end-devices (non-scheduled devices cannot communicate until they are scheduled), their allocated SF and transmission power. For a duty cycle of $d\%$, the inter-beacon time is divided into $100/d$ scheduling periods, i.e., 10 scheduling periods for a duty cycle of 10% and 100 for a duty cycle of 1%. Thus, each node is allowed to transmit during only one scheduling period within each inter-beacon time. To ensure this duty cycle, the proposed algorithm is run for each scheduling period p, where the candidate devices for allocation is $\mathcal{N} \setminus \bigcup_{i=1}^{p-1} \mathcal{N}_i$, where $\mathcal{N}$ is the set of all devices and $\mathcal{N}_i$ is the set of devices allocated in period i. Hence, in order to avoid wasting time, the duration between two beacons should be equal to an integer number of slots, for all SFs. This is possible either by making the slots of different SFs contain the same number of symbols but not the same number of bits as an SF m symbol has m bits (in this case, the number of slots for SF $m < 12$ is equal to $2^{12-m} \times n_{\text{slots},12}$), or by making the slots of different SFs correspond to the same number of bits (in this case, it can be shown that a sufficient condition to get integer values of all $n_{\text{slots},m}$ is to define $n_{\text{slots},12}$ as a multiple of 6). Note that the impact of this beacon overhead and of the slots' guard intervals can be assumed negligible.

IV. PROBLEM FORMULATION

In this section, we formulate the joint SF and power allocation optimization problem in our considered LoRa-based system, under imperfect SF orthogonality. In particular, the goal will be to improve the overall fairness of the system by maximizing the minimal uplink average rate over end-devices and SFs, under co-SF and inter-SF interferences. We first derive the expression of the probability of successful reception, $P_{\text{cap}}^{(n,m)}$. Assuming $N > 1$, there are two cases:

1) One End-Device n at SF m: end-device n is only subject to inter-SF interferences. The transmission can be successfully decoded if the node satisfies the *inter-SF* as well as the *signal reception* conditions. In this case, inter-SF interferences are more critical than the signal reception condition since there are always inter-SF interferences for $N > 1$. Hence the probability of successful transmission can be written as,

$$P_{\text{cap}_{\text{iSF}}}^{(n,m)} = P\left(\text{SINR}_{nm}^{\text{inter}} \geq \tilde{\theta}_m\right), \tag{7}$$

where $\text{SINR}_{nm}^{\text{inter}}$ is given in (4) and $\tilde{\theta}_m$ is the inter-SF interference capture threshold for SF m, defined in Table I. Using the random instantaneous CNR variables ζ_n for all n and marginalizing over them, it is shown in [1] with similar

calculations as in [11] that (7) can be written as,

$$P_{\text{cap}_{\text{iSF}}}^{(n,m)} = e^{-\frac{\tilde{\theta}_m \sigma_c^2 r_n^\alpha}{A(f_c) p_{nm}}} \prod_{i \in \mathcal{N}_{-n}} \prod_{j \in \mathcal{M}_{-m}} \frac{1}{\tilde{\theta}_m s_{ij} \frac{p_{ij}}{p_{nm}} \times (\frac{r_n}{r_i})^\alpha + 1}. \tag{8}$$

2) More Than One End-Device at SF m: in this case, the co-SF interferences, as well as the inter-SF interferences, largely dominate the signal reception condition [11]. Therefore, the success probability is expressed as in [20],

$$P_{\text{cap}_{\text{coSF}}}^{(n,m)} = P\left(\text{SINR}_{nm}^{\text{co}} \geq \theta_{\text{co}}\right), \tag{9}$$

where $\text{SINR}_{nm}^{\text{co}}$ is given in (5) and θ_{co} is the co-SF capture threshold which is equal to 6dB for all SF m [6], [20]. With similar calculations as in [1], we obtain

$$P_{\text{cap}_{\text{coSF}}}^{(n,m)}$$

$$= \left(\prod_{i \in \mathcal{N}_{-n}} \prod_{j \in \mathcal{M}_{-m}} \frac{1}{\theta_{\text{co}} s_{ij} \frac{p_{ij}}{p_{nm}} \times \left(\frac{r_n}{r_i}\right)^\alpha + 1}\right)$$

$$\times e^{-\frac{\theta_{\text{co}} \sigma_c^2 r_n^\alpha}{A(f_c) p_{nm}}} \times \prod_{i \in \mathcal{N}_{-n}} \frac{1}{\theta_{\text{co}} s_{im} \frac{p_{im}}{p_{nm}} \times \left(\frac{r_n}{r_i}\right)^\alpha + 1}. \tag{10}$$

Given the above analysis, the joint SF and transmit power allocation optimization underlying LoRaWAN network is formulated as follows (for $N > 1$),

$$\max_{s_{nm} p_{nm}} \min_{\substack{(n,m)\in \\ \mathcal{N}\times\mathcal{M} \\ \text{s.t. } s_{nm}\neq 0}} f(s_{nm}, p_{nm}) = s_{nm} R_m P_{\text{cap}}^{(n,m)}, \tag{11}$$

namely maximizing the minimum end-device rate after co-SF and inter-SF capture, where the minimization is over the s_{nm} that are non-zero, and

$$P_{\text{cap}}^{(n,m)} = I\left(\sum_{k\in\mathcal{N}} s_{km} \geq 2\right) P_{\text{cap}_{\text{coSF}}}^{(n,m)}$$

$$+ I\left(\sum_{k\in\mathcal{N}} s_{km} = 1\right) P_{\text{cap}_{\text{iSF}}}^{(n,m)}, \tag{12}$$

where $I(C)$ is the indicator function, i.e., it equals 1 if the condition C is verified and 0 otherwise.

Finally, the overall optimization problem[1] becomes

$$(P) \max_{s_{nm} p_{nm}} \min_{\substack{(n,m)\in \\ \mathcal{N}\times\mathcal{M}\,\text{s.t. } s_{nm}\neq 0}} f(s_{nm}, p_{nm})$$

$$= s_{nm} R_m$$

$$\times \left[I\left(\sum_{k\in\mathcal{N}} s_{km} = 1\right) P_{\text{cap}_{\text{iSF}}}^{(n,m)}\right.$$

$$\left. + I\left(\sum_{k\in\mathcal{N}} s_{km} \geq 2\right) P_{\text{cap}_{\text{coSF}}}^{(n,m)}\right] \tag{13}$$

s.t. C1: $0 \leq p_{nm} \leq P_{\max}, p_{nm} \in \mathbb{R}^+$ (13a)

C2: $s_{nm} \in \{0,1\}, \forall(n,m) \in \mathcal{N} \times \mathcal{M}$ (13b)

C3: $\sum_{m\in\mathcal{M}} s_{nm} \leq 1, \forall n \in \mathcal{N}$ (13c)

[1]Without loss of generality, the description is for the first scheduling frame of an inter-beacon period. In subsequent frames, the same problem is solved but over the remaining unscheduled devices.

$$\text{C4:} \sum_{n \in \mathcal{N}} s_{nm} \leq \text{N}_{\max}(m), \ \forall m \in \mathcal{M} \tag{13d}$$

$$\text{C5:} \ \text{if } N > M, 1 \leq \sum_{n \in \mathcal{N}} s_{nm}, \ \forall m \in \mathcal{M} \tag{13e}$$

where, from (8) and (10), the objective (13) can be developed as

$$
\begin{aligned}
&f(s_{nm}, p_{nm}) \\
&= s_{nm} R_m \Bigg[I \left(\sum_{k \in \mathcal{N}} s_{km} = 1 \right) e^{-\frac{\tilde{\theta}_m \sigma_c^2 r_n^\alpha}{A(f_c) p_{nm}}} \\
&\quad \times \prod_{i \in \mathcal{N}_{-n}} \prod_{j \in \mathcal{M}_{-m}} \frac{1}{\tilde{\theta}_m s_{ij} \frac{p_{ij}}{p_{nm}} \left(\frac{r_n}{r_i} \right)^\alpha + 1} \\
&\quad + I \left(\sum_{k \in \mathcal{N}} s_{km} \geq 2 \right) \\
&\quad \times e^{-\frac{\theta_{\text{co}} \sigma_c^2 r_n^\alpha}{A(f_c) p_{nm}}} \left(\prod_{i \in \mathcal{N}_{-n}} \prod_{j \in \mathcal{M}_{-m}} \frac{1}{\theta_{\text{co}} s_{ij} \frac{p_{ij}}{p_{nm}} \left(\frac{r_n}{r_i} \right)^\alpha + 1} \right) \\
&\quad \times \prod_{i \in \mathcal{N}_{-n}} \frac{1}{\theta_{\text{co}} s_{im} \frac{p_{im}}{p_{nm}} \left(\frac{r_n}{r_i} \right)^\alpha + 1} \Bigg]. \tag{14}
\end{aligned}
$$

Our objective function (13) expresses the maximization of the minimum data-rate over all served end-devices (i.e., for which $s_{nm} \neq 0$) and SFs. Constraint (13a) is the power budget, where the maximum transmit power per end-device is fixed to $P_{\max}$. Constraint (13b) defines the binary SF allocation variables s_{nm}. Constraints (13c) and (13d)[2] ensure that an end-device n is assigned to at most one SF, and that the maximal number of end-devices sharing SF m is $\text{N}_{\max}(m)$. This means that $N - \sum_{m \in \mathcal{M}} \text{N}_{\max}(m)$ end-devices will be turned-off, however, they will be activated in subsequent scheduling periods when they experience better channel conditions. Finally, constraint (13e) ensures that if there are enough end-devices ($N > M$), no SFs should remain unused, i.e., at least one end-device should be allocated to each SF. Clearly, (P) is a mixed-integer problem with a non-convex objective function, as it includes both binary allocation variables s_{nm} and continuous power allocation variables p_{nm}. Such problems are known to be generally NP-hard [21], making them difficult to solve. We thus, propose to solve this problem by decomposing it into the following two optimization phases: (1) the discrete optimization phase of the allocation of binary variables s_{nm} while keeping the power allocation variables p_{nm} fixed to $P_{\max}$, (2) the continuous optimization phase of the power allocation variables p_{nm}, where the allocation variables have been fixed to their previous solution. These two phases may be iterated until convergence, or until the maximum number of iterations N_I is reached.

Denoting by $\mathbf{s} = [s_{nm}]$ and $\mathbf{p} = [p_{nm}], \forall n \in \mathcal{N}, m \in \mathcal{M}$, the SF assignment and transmit power vectors, respectively, Alg. 1 provides the overview of the general proposal.

Algorithm 1 Proposed SF and Transmit Power Allocation

Initialization: SF assignment vector: $\mathbf{s}^{(0)} \leftarrow \mathbf{0}$, transmit power vector: $\mathbf{p}^{(0)} \leftarrow P_{\max}$.
1: $i \leftarrow 1$.
2: **do**
3:      SF assignment: find $\mathbf{s}^{(i)}$, for fixed $\mathbf{p}^{(i-1)}$.   ▷ (Sec. V)
4:      Transmit power allocation: find $\mathbf{p}^{(i)}$, for fixed $\mathbf{s}^{(i)}$.   ▷ (Sec. VI)
5:      $i \leftarrow i + 1$.
6: **while** $f\left(\mathbf{s}^{(i)}, \mathbf{p}^{(i)}\right) - f\left(\mathbf{s}^{(i-1)}, \mathbf{p}^{(i-1)}\right) \geq \epsilon$ or $i \leq N_I$.

In the next sections, we describe each of the optimization phases.

V. PROPOSED SPREADING FACTOR ALLOCATION

A. Formulation of the Proposed SF Allocation Optimization

In this subsection, the problem of SF allocation is addressed. We assume that all end-devices transmit with the maximum transmission power, i.e., $p_{nm} = P_{\max}, \forall n, m$. This problem can be formulated as follows,

$$
\begin{aligned}
(P1) \max_{s_{nm}} & \min_{\substack{(n,m) \in \\ \mathcal{N} \times \mathcal{M} \text{ s.t. } s_{nm} \neq 0}} f(s_{nm}) = s_{nm} R_m \\
& \times \Bigg[I \left(\sum_{k \in \mathcal{N}} s_{km} \geq 2 \right) P_{\text{cap}_{\text{coSF}}}^{(n,m)} \\
& + I \left(\sum_{k \in \mathcal{N}} s_{km} = 1 \right) P_{\text{cap}_{\text{iSF}}}^{(n,m)} \Bigg]
\end{aligned} \tag{15}
$$

$$\text{s.t. C1:} \ s_{nm} \in \{0, 1\}, \ \forall (n, m) \in \mathcal{N} \times \mathcal{M} \tag{15a}$$

$$\text{C2:} \sum_{m \in \mathcal{M}} s_{nm} \leq 1, \ \forall n \in \mathcal{N} \tag{15b}$$

$$\text{C3:} \sum_{n \in \mathcal{N}} s_{nm} \leq \text{N}_{\max}(m), \ \forall m \in \mathcal{M} \tag{15c}$$

$$\text{C4:} \ \text{if } N > M, 1 \leq \sum_{n \in \mathcal{M}} s_{nm}, \ \forall m \tag{15d}$$

where $f(s_{nm}) = f(s_{nm}, p_{nm} = P_{\max})$ in (15), and hence from (14), is given by

$$
\begin{aligned}
f(s_{nm}) &= s_{nm} R_m \Bigg[I \left(\sum_{k \in \mathcal{N}} s_{km} \geq 2 \right) e^{-\frac{\theta_{\text{co}} \sigma_c^2 r_n^\alpha}{A(f_c) P_{\max}}} \\
&\quad \times \prod_{i \in \mathcal{N}_{-n}} \frac{1}{\theta_{\text{co}} s_{im} \left(\frac{r_n}{r_i} \right)^\alpha + 1} \\
&\quad + I \left(\sum_{k \in \mathcal{N}} s_{km} = 1 \right) e^{-\frac{\tilde{\theta}_m \sigma_c^2 r_n^\alpha}{A(f_c) P_{\max}}} \\
&\quad \times \prod_{\substack{(i,j) \in \\ \mathcal{N}_{-n} \times \mathcal{M}_{-m}}} \frac{1}{\tilde{\theta}_m s_{ij} \left(\frac{r_n}{r_i} \right)^\alpha + 1} \Bigg]. \tag{16}
\end{aligned}
$$

$(P1)$ is an integer programming problem, given the binary variables s_{nm}, with a non-linear objective function, hence it is difficult to obtain its optimal solution. Therefore, we propose

---

[2]Problem (13) also holds without C4, but would entail large computational burden for large N as shown in Proposition 3, while in practice, only small $\text{N}_{\max}(m)$ are viable due to co-SF interferences, as shown in Table II.

an optimized SF allocation method, using tools from matching theory.

Matching theory is a promising tool for resource allocation in wireless networks [22]. According to this theory, our considered allocation problem $(P1)$ can be classified as a many-to-one matching problem with conventional externalities and peer effects. There are two sets of players, the set of SFs and the set of end-devices, where each player of the one set seeks to be matched with players of the opposing set. An end-device prefers to be matched to the SF offering the highest utility, while each SF prefers to be matched with the group of end-devices with the highest utility. The difficulty of our problem is that there is an interdependency between nodes' preferences, i.e., whenever an end-device is matched to an SF, the preferences of the other end-devices may change due to co-SF and inter-SF interferences. In addition to these conventional externalities (preference interdependency) and unlike the problem in [12] where only orthogonal channels (not SFs) were considered, our problem exhibits peer effects that are caused by inter-SF interferences. That is, the preferences of an end-device depend not only on the identity of the SF and the number of end-devices assigned to it, but also on the assignment of end-devices to other SFs (since they cause inter-SF interferences). Therefore, to solve $(P1)$, we propose a many-to-one matching algorithm between the set $\mathcal{M}$ of SFs and the set $\mathcal{N}$ of end-devices. Next, we define the basic concepts of matching theory.

B. Fundamentals of Matching Theory

To describe our proposed matching-based algorithm, we first present the basic concepts of matching theory that have been used in our algorithm:

- **Matching pair:** a couple (n, m) assigned to each other.
- **Quotas of a player:** the maximum number of players with which it can be matched
  - Each end-device has a quota of 1 (15b),
  - Each SF m has a quota of $\mathrm{N_{max}}(m)$ end-devices (15c).
- **Utility of an end-device:** defined for our problem as its short-term average rate. If it is the only end-device at SF m,

$$U_n = R_m e^{-\frac{\tilde{\theta}_m \sigma_c^2 r_n^\alpha}{\mathrm{A}(f_c) P_{\max}}} \prod_{i \in \mathcal{N}_{-n}} \prod_{j \in \mathcal{M}_{-m}} \frac{1}{\tilde{\theta}_m s_{ij}\left(\frac{r_n}{r_i}\right)^\alpha + 1}. \quad (17)$$

If it shares the SF m with other end-devices,

$$U_n = R_m e^{-\frac{\theta_{\mathrm{co}} \sigma_c^2 r_n^\alpha}{\mathrm{A}(f_c) P_{\max}}} \prod_{i \in \mathcal{N}_{-n}}$$
$$\times \prod_{j \in \mathcal{M}_{-m}} \frac{1}{\theta_{\mathrm{co}} s_{ij}\left(\frac{r_n}{r_i}\right)^\alpha + 1}$$
$$\times \prod_{i \in \mathcal{N}_{-n}} \frac{1}{\theta_{\mathrm{co}} s_{im}\left(\frac{r_n}{r_i}\right)^\alpha + 1}. \quad (18)$$

- **Utility of an SF:** defined for our problem as the minimum short-term average rate among the end-devices assigned

to it. If SF m is matched to one end-device only:

$$U_m = R_m e^{-\frac{\tilde{\theta}_m \sigma_c^2 r_n^\alpha}{\mathrm{A}(f_c) P_{\max}}} \prod_{i \in \mathcal{N}_{-n}} \prod_{j \in \mathcal{M}_{-m}} \frac{1}{\tilde{\theta}_m s_{ij}\left(\frac{r_n}{r_i}\right)^\alpha + 1}, \quad (19)$$

otherwise U_m is given as

$$U_m = \min_{n \in \mathcal{A}_m} R_m e^{-\frac{\theta_{\mathrm{co}} \sigma_c^2 r_n^\alpha}{\mathrm{A}(f_c) P_{\max}}}$$
$$\times \prod_{i \in \mathcal{N}_{-n}} \prod_{j \in \mathcal{M}_{-m}} \frac{1}{\theta_{\mathrm{co}} s_{ij}\left(\frac{r_n}{r_i}\right)^\alpha + 1}$$
$$\times \prod_{i \in \mathcal{N}_{-n}} \frac{1}{\theta_{\mathrm{co}} s_{im}\left(\frac{r_n}{r_i}\right)^\alpha + 1}, \quad (20)$$

where $\mathcal{A}_m$ is the set of end-devices assigned to SF m.
- **Preference relation**: a player q prefers a player p_1 over the player p_2, if the utility of q is higher when it is matched to p_1 than when it is matched to p_2.
- **Blocking pair:** a matching pair (n, m) is a blocking pair when U_n or U_m is higher when n uses m, than when they use their current matches, without lowering the utilities of any other end-device nor SF. In this case, n will leave its current match to be matched to m.
- **Two-sided exchange stable matching:** a matching solution where there is no blocking pair.

Algorithm 2 Initial Matching

Initialization: Set of unmatched end-devices: $\mathcal{L}_U \leftarrow \mathcal{N}$, $\mathcal{A}_m \leftarrow \emptyset$

1: **while** $\mathcal{L}_U \neq \emptyset$ **do**
2:     **for** $i \in \mathcal{L}_U$ **do**
3:         **if** $\mathcal{L}_{p,i} = \emptyset$ **then**
4:             $\mathcal{L}_U \leftarrow \mathcal{L}_U \backslash \{i\}$;
5:         **else**
6:             $a \leftarrow \mathrm{firstPrefered}(\mathcal{L}_{p,i})$;   ▷ Favorite SF
7:             $\mathcal{L}_{p,i} \leftarrow \mathcal{L}_{p,i} \backslash \{a\}$;
8:             $\mathrm{req}_a \leftarrow \mathrm{req}_a \cup \{i\}$;
9:     **for** $j \in \mathcal{M}$ **do**
10:        **if** $size(\mathrm{req}_j) > 0$ & $size(\mathcal{A}_j) < \mathrm{N_{max}}(j)$ **then**
11:          **if** $(size(\mathrm{req}_j) + size(\mathcal{A}_j)) \leq \mathrm{N_{max}}(j)$ **then**
12:             Accept all the requests and add the end-devices to $\mathcal{A}_j$;
13:          **else**
14:             Accept the requests of the $(\mathrm{N_{max}} - size(\mathcal{A}_j))$ most preferred end-devices;
15:             Add them to $\mathcal{A}_j$;

C. Proposed SF-Allocation Algorithm

In this subsection, we describe the steps of the proposed matching-based algorithm which exploits matching techniques as in [12], [22], tailored to our specific problem. First, the gateway performs an initial matching between the set $\mathcal{M}$ of SFs and the set $\mathcal{N}$ of end-devices by the Initial Matching in Algorithm 2. Next, it swaps the matching pairs obtained in

Algorithm 3 Matching Refinement
1: change←true;
2: **while** change = true **do**
3:    change←false;
4:    **for** $j \in \mathcal{M}$ **do**
5:       Calculate U_j;   ▷ eq. (19) or eq. (20)
6:       **for** $i \in \mathcal{A}_j$ **do**
7:          Calculate U_i;   ▷ eq. (17) or eq. (18)
8:          **for** $l \in \mathcal{M}_{-j}$ **do**
9:             **if** $size(\mathcal{A}_l) = 0$ **then**
10:                Swap$\big((i,j),(\emptyset,l)\big)$;
11:                Calculate the new utility U'_i of i; ▷ eq. (17)
                      or eq. (18)
12:                **if** $U'_i \geq U_i$ **then**
13:                   Validate the Swap;
14:                   change ← true;
15:             **else**
16:                Calculate U_l;   ▷ eq. (19) or eq. (20)
17:                **for** $k \in \mathcal{A}_l$ **do**
18:                   Calculate U_k;   ▷ eq. (17) or eq. (18)
19:                   Swap$\big((i,j),(k,l)\big)$;
20:                   **if** (i,l) or (k,j) is a blocking pair **then**
21:                      Validate the Swap;
22:                      change ← true;

the previous step until reaching a two-sided exchange stable matching by the Matching Refinement in Algorithm 3. Details of these steps are given below.

Let $\mathcal{L}_U$ denote the set of end-devices that are not allocated to any SF, req_m the requests received by SF m, and $\mathcal{A}_m$ the set of end-devices assigned to SF m. We suppose that the gateway knows its distance with all end-devices.

Initialization: the gateway starts by initializing the preference lists of end-devices and SFs. Each end-device n with a distance r_n to the gateway, can only use SFs if they are included in the coverage area ($r_n \leq l_m$) of the gateway for these SFs, therefore,

$$\mathcal{L}_{p,n} = \{m \in \mathcal{M}, \text{ s.t. } r_n \leq l_m\}. \quad (21)$$

$\mathcal{L}_{p,n}$ is sorted according to the increasing order of the distance threshold of the SFs (l_m, $m \in \mathcal{M}$), i.e., an SF with higher achievable rate is preferred. On the other hand, SF m only considers end-devices having a distance to the gateway lower than l_m,

$$\mathcal{L}_{p,m} = \{n \in \mathcal{N}, \text{ s.t. } r_n \leq l_m\}. \quad (22)$$

$\mathcal{L}_{p,m}$ is ordered such that a user $n_1 \in \mathcal{L}_{p,m}$ is ranked before another user $n_2 \in \mathcal{L}_{p,m}$ if n_1 is located in the ring of SF m ($n_1 \in (l_{m-1}, l_m]$) but not n_2 ($n_2 \notin (l_{m-1}, l_m]$), or both are in the ring of SF m but n_1 is closer to the gateway than n_2 ($|r_{n_1}| < |r_{n_2}|$).

Unmatched end-devices are added to $\mathcal{L}_U$.

Initial Matching: for each end-device n in the unmatched list $\mathcal{L}_U$, if $\mathcal{L}_{p,n} \neq \emptyset$, n requests its first preferred SF and removes it from $\mathcal{L}_{p,n}$, otherwise the end-device is removed from $\mathcal{L}_U$ since all SFs it can use have already reached their

quota. Then, each SF m either accepts all current requests if its quota allows it, or it accepts the requests of its most preferred end-devices that fulfill its quota, if not. This process is repeated until $\mathcal{L}_U$ becomes empty.

Matching Refinement: for each matching pair (n, m), the algorithm calculates U_m using (19) if it is only assigned to end-device n and (20) in the other case. The utility of end-device n is calculated by (17) if it is the only one at SF m, and with (18) otherwise. Firstly, if there is an SF l that is not assigned to any end-device that allows to increase U_n, the end-device leaves SF m to be matched with SF l. Then, the algorithm calculates the utilities of every pair (k, l), and makes a swap between (n, m) and (k, l) and determines their new utilities. Secondly, if (k, m) or (n, l) is a blocking pair, the algorithm makes a swap. This swapping step is repeated until reaching a two-sided exchange stable matching.

D. Proposed SF-Allocation Algorithm Analysis

For our proposed SF-Allocation algorithm we have the following theorems. The proofs and the details of the computational complexity analysis are presented in Appendix A.

Proposition 1 (Stability): When the proposed algorithm terminates, it finds a two-sided exchange stable matching.

Proposition 2 (Convergence): After a finite number of swap operations, the algorithm eventually converges to a two-sided exchange stable matching.

Proposition 3 (Complexity): The running time of our proposed algorithm is upper-bounded by $\mathcal{O}\left(NM + Q^2 M^2\right)$, where $Q = \max\limits_{m \in \mathcal{M}} \{N_{\max}(m)\}$.

Since M and Q are generally small as, e.g., in LoRaWAN ($M = 6$ in LoRaWAN, and we will later see in Table II that we suggest to use $Q \leq 3$), the complexity is essentially linear in the number of end-devices N. Hence, we believe that the complexity of the matching algorithm will not be a limiting factor in a real LoRa-based network, as it runs on the network server which has extensive computation capabilities (unlike end-devices or even gateways).

VI. PROPOSED POWER ALLOCATION OPTIMIZATION

Once the end-devices are assigned to SFs, we next optimize the power allocation variables in order to maximize the minimal throughput achieved on each SF. Let $\mathcal{N}_j$ be the set of end-devices assigned to SF j. Given the assignment variable solutions denoted $s^*_{nm}, \forall n, m$ solved by the previous step, the power allocation problem can be written as follows,

$$\max_{p_{nm}} \min_{\substack{(m,n) \in \\ \mathcal{M} \times \mathcal{N}_m}} f(p_{nm})$$

$$= R_m \left[I\left(\sum_{k \in \mathcal{N}_m} s^*_{km} = 1 \right) P^{(n,m)}_{\text{cap}_{\text{iSF}}} \right.$$

$$\left. + I\left(\sum_{k \in \mathcal{N}_m} s^*_{km} \geq 2 \right) P^{(n,m)}_{\text{cap}_{\text{coSF}}} \right] \quad (23a)$$

$$\text{s.t. C1: } 0 \leq p_{nm} \leq P_{\max}, p_{nm} \in \mathbb{R}^+ \quad (23b)$$

where $f(p_{nm}) = f(s^*_{nm}, p_{nm})$ in (14).

It can be observed that the objective function $f(p_{nm})$ of problem (23), unlike in previous works such as [12], is non-linear non-convex, for which a global optimum is difficult to obtain. This greatly increases the difficulty of this optimization problem. Instead, we seek for a near-optimal solution by transforming the initial problem as follows. Let $\mathcal{P}_\eta$ be the set of transmit power vectors $\mathbf{p}$ such that the minimum throughput over end-devices and SFs is above a certain parameter $\eta \in \mathbb{R}^+$, namely

$$\mathcal{P}_\eta = \left\{ \mathbf{p} \,\middle|\, \min_m f(p_{nm}) \geq \eta, \forall n \in \mathcal{N}_m \right\}. \quad (24)$$

Since the minimal throughput value is above η, all throughput values should be above η as well. Hence, defining

$$\mathcal{P}_\eta^* = \left\{ \mathbf{p} \,|\, f(p_{nm}) \geq \eta, \forall m \in \mathcal{M}, \forall n \in \mathcal{N}_m \right\}, \quad (25)$$

we can write $\mathcal{P}_\eta^* = \mathcal{P}_\eta$. Problem (23) is hence, equivalent to the following optimization problem,

$$\max_{p_{nm}, \eta} \eta \quad (26)$$
$$\text{s.t. C1: } 0 \leq p_{nm} \leq P_{\max}, p_{nm} \in \mathbb{R}^+ \quad (26a)$$
$$\text{C2: } \mathbf{p} \in \mathcal{P}_\eta^* \quad (26b)$$

Therefore, we take the following approach: for a given η, we solve the feasibility problem

$$\text{Find } \mathbf{p} \quad (27)$$
$$\text{s.t. } \mathbf{p} \in [0, P_{\max}]^{NM \times 1} \cap \mathcal{P}_\eta^*, \quad (27a)$$

then η is increased until no feasible $\mathbf{p}$ can be found. In practice, parameter η can be updated using the bisection method [12] as detailed in Algorithm 4, as follows. Initially, η is lower-bounded by $\eta_{\min} = 0$, upper-bounded by $\eta_{\max}$ which is equal to the minimal bit-rate over allocated SFs and end-devices. First, setting η as the midpoint of the interval $[\eta_{\min}, \eta_{\max}]$, problem (27) is solved and if a feasible solution is found, it is denoted as $\mathbf{p}_{opt}$ and we update the lower bound $\eta_{\min}$ as η. Otherwise, if no feasible power vector is found, $\eta_{\max}$ is set as η. This procedure is iterated until the interval length $[\eta_{\min}, \eta_{\max}]$ is smaller than the desired accuracy ϵ.

Algorithm 4 Power allocation optimization

Initialization: $\eta_{\min} \leftarrow 0$, $\eta_{\max} \leftarrow \min_{m \in \mathcal{M}} R_m$, $\epsilon > 0$.

1: **while** $\eta_{\max} - \eta_{\min} \geq \epsilon$ **do**
2: $\quad \eta \leftarrow \frac{(\eta_{\max} + \eta_{\min})}{2}$;
3: $\quad$ Solve (27): find a transmit power vector $\mathbf{p}$ satisfying the constraint in (27);
4: $\quad$ **if** $\mathbf{p}$ exists **then**
5: $\quad\quad \mathbf{p}_{opt} \leftarrow \mathbf{p}$;
6: $\quad\quad$ Calculate the utilities of each SF m, U_m using $\mathbf{p}_{opt}$
7: $\quad\quad \eta_{\min} \leftarrow \eta$;
8: $\quad$ **else**
9: $\quad\quad \eta_{\max} \leftarrow \eta$;
10: $\mathcal{P}_\eta^* \leftarrow \mathbf{p}_{opt}$;

However, $\mathcal{P}_\eta^*$ contains non-linear inequalities, making it difficult to solve the feasibility problem (27). Hence, we devise two methods for making this problem tractable: linear approximation in Subsection VI-A, and quadratic approximation in Subsection VI-B.

A. Feasibility Problem With Linear Approximation

In order to make problem (27) tractable, we first approximate the non-linear inequalities in the set $\mathcal{P}_\eta^*$ by linear ones. We distinguish two cases, one where only a single end-device is assigned to SF m and the second, where more than one end-devices are assigned to SF m.

1) Case 1: a single end-device n is assigned to SF m, hence n is only subject to inter-SF interferences. Therefore, given (8), $\mathcal{P}_\eta^*$ is given by,

$$\mathcal{P}_\eta^* = \left\{ \mathbf{p} \,\middle|\, R_m \mathrm{e}^{-\frac{\tilde{\theta}_m \sigma_c^2 r_n^\alpha}{A(f_c) p_{nm}}} \right.$$
$$\times \prod_{j \in \mathcal{M}_{-m}} \prod_{i \in \mathcal{N}_{j-n}} \frac{1}{\tilde{\theta}_m \frac{p_{ij}}{p_{nm}} \left(\frac{r_n}{r_i}\right)^\alpha + 1} \geq \eta,$$
$$\left. \vphantom{\prod} \forall m \in \mathcal{M} \right\}. \quad (28)$$

Rearranging and taking the logarithm of both sides, the inequalities in (28) are equivalent to

$$\frac{\tilde{\theta}_m \sigma_c^2 r_n^\alpha}{A(f_c) p_{nm}} + \sum_{j \in \mathcal{M}_{-m}} \sum_{i \in \mathcal{N}_{j-n}} \ln\left(\tilde{\theta}_m \frac{p_{ij}}{p_{nm}} \left(\frac{r_n}{r_i}\right)^\alpha + 1\right)$$
$$\leq -\ln\left(\frac{\eta}{R_m}\right), \quad \forall m \in \mathcal{M}. \quad (29)$$

In Appendix B.1, we prove that the inequality in $\mathcal{P}_\eta^*$ can be approximated as follows,

$$\ln\left(\frac{\eta}{R_m}\right) p_{nm} + \sum_{j \in \mathcal{M}_{-m}} \sum_{i \in \mathcal{N}_{j-n}} \tilde{\theta}_m \left(\frac{r_n}{r_i}\right)^\alpha p_{ij}$$
$$\leq -\frac{\tilde{\theta}_m \sigma_c^2 r_n^\alpha}{A(f_c)}, \quad \forall m \in \mathcal{M}. \quad (30)$$

2) Case 2: if SF m is shared by more than one end-device, from (10), the set $\mathcal{P}_\eta^*$ is given by

$$\mathcal{P}_\eta^*$$
$$= \left\{ \mathbf{p} \,\middle|\, R_m \mathrm{e}^{-\frac{\theta_{\mathrm{co}} \sigma_c^2 r_n^\alpha}{A(f_c) p_{nm}}} \left(\prod_{j \in \mathcal{M}_{-m}} \prod_{i \in \mathcal{N}_{j-n}} \frac{1}{\theta_{\mathrm{co}} \frac{p_{ij}}{p_{nm}} \left(\frac{r_n}{r_i}\right)^\alpha + 1} \right) \right.$$
$$\left. \times \prod_{i \in \mathcal{N}_{m-n}} \frac{1}{\theta_{\mathrm{co}} \frac{p_{im}}{p_{nm}} \left(\frac{r_n}{r_i}\right)^\alpha + 1} \geq \eta, \quad \forall m \in \mathcal{M} \right\}. \quad (31)$$

Similarly to Case 1, the inequality in $\mathcal{P}_\eta^*$ can be approximated as, (see Appendix B.2)

$$\frac{\theta_{\mathrm{co}} \sigma_c^2 r_n^\alpha}{A(f_c) p_{nm}} + \left(\sum_{j \in \mathcal{M}_{-m}} \sum_{i \in \mathcal{N}_{j-n}} \ln(2) - \frac{1}{2} + \frac{\theta_{\mathrm{co}}}{2} \left(\frac{r_n}{r_i}\right)^\alpha \frac{p_{ij}}{p_{nm}} \right)$$
$$+ \sum_{i \in \mathcal{N}_{m-n}} \ln(2) - \frac{1}{2} + \frac{\theta_{\mathrm{co}}}{2} \left(\frac{r_n}{r_i}\right)^\alpha \frac{p_{im}}{p_{nm}} \leq -\ln\left(\frac{\eta}{R_m}\right). \quad (32)$$

Finally, from (30) and (32), problem (27) can be expressed as,

$$\text{Find } \mathbf{p} \quad (33)$$
$$\text{s.t. C1: } 0 \leq p_{nm} \leq P_{\max} \quad (33a)$$

$$\text{C6: } \ln\left(\frac{\eta}{R_m}\right)p_{nm} + \frac{\tilde{\theta}_m\sigma_c^2 r_n^\alpha}{A(f_c)} + \tag{33b}$$

$$\sum_{j\in\mathcal{M}_{-m}}\sum_{i\in\mathcal{N}_{j-n}}\tilde{\theta}_m\left(\frac{r_n}{r_i}\right)^\alpha p_{ij} \le 0, \text{ if } \sum_{k\in\mathcal{N}_m}s_{km}^* = 1$$

$$\text{C7: } \ln\left(\frac{\eta}{R_m}\right)p_{nm} + \frac{\theta_{\text{co}}\sigma_c^2 r_n^\alpha}{A(f_c)}$$

$$+ \left(\sum_{j\in\mathcal{M}_{-m}}\sum_{i\in\mathcal{N}_{j-n}}\left(\ln(2) - \frac{1}{2}\right)p_{nm}\right.$$

$$\left. + \frac{\theta_{\text{co}}}{2}\left(\frac{r_n}{r_i}\right)^\alpha p_{ij}\right)$$

$$+ \sum_{i\in\mathcal{N}_{m-n}}\left(\ln(2) - \frac{1}{2}\right)p_{nm} + \frac{\theta_{\text{co}}}{2}\left(\frac{r_n}{r_i}\right)^\alpha p_{im} \le 0,$$

$$\text{if } \sum_{k\in\mathcal{N}_m}s_{km}^* \ge 2 \tag{33c}$$

Although problem (33) is a feasibility problem, by taking an arbitrary objective function, it can be written as a linear programming problem defined by linear inequalities. Hence, it can be solved with usual linear programming solvers such as *linprog* or *fmincon* in Matlab.

B. Feasibility Problem With Quadratic Approximation

In this subsection, we propose a second method for making problem (27) tractable, by means of quadratic approximation of the non-linear inequalities of $\mathcal{P}_\eta^*$. As in the previous subsection, we distinguish two cases:

1) Case 1: only one end-device assigned to SF m. $\mathcal{P}_\eta^*$ is equal to (28). The quadratic approximation of the logarithmic terms in (29) using the Taylor-Maclaurin series, is given by

$$\ln\left(\tilde{\theta}_m\frac{p_{ij}}{p_{nm}}\left(\frac{r_n}{r_i}\right)^\alpha + 1\right)$$

$$= \tilde{\theta}_m\frac{p_{ij}}{p_{nm}}\left(\frac{r_n}{r_i}\right)^\alpha$$

$$- \frac{\tilde{\theta}_m^2}{2}\left(\frac{p_{ij}}{p_{nm}}\right)^2\left(\frac{r_n}{r_i}\right)^{2\alpha} + o\left(\tilde{\theta}_m^2\left(\frac{p_{ij}}{p_{nm}}\right)^2\left(\frac{r_n}{r_i}\right)^{2\alpha}\right). \tag{34}$$

Substituting the logarithmic term in (29) and rearranging, we obtain the following inequality,

$$\ln\left(\frac{\eta}{R_m}\right)p_{nm}^2 + \frac{\tilde{\theta}_m\sigma_c^2 r_n^\alpha}{A(f_c)}p_{nm}$$

$$+ \sum_{j\in\mathcal{M}_{-m}}\sum_{i\in\mathcal{N}_{j-n}}\tilde{\theta}_m\left(\frac{r_n}{r_i}\right)^\alpha p_{ij}p_{nm}$$

$$- \frac{\tilde{\theta}_m^2}{2}\left(\frac{r_n}{r_i}\right)^{2\alpha}p_{ij}^2 \le 0. \tag{35}$$

2) Case 2: SF m is shared by more than one end-device. $\mathcal{P}_\eta^*$ is given by (31).

Similarly, the inequality in $\mathcal{P}_\eta^*$ can be approximated as, (see Appendix C)

$$\ln\left(\frac{\eta}{R_m}\right)p_{nm}^2 + \frac{\theta_{\text{co}}\sigma_c^2 r_n^\alpha}{A(f_c)}p_{nm}$$

$$+ \left(\sum_{j\in\mathcal{M}_{-m}}\sum_{i\in\mathcal{N}_{j-n}}\left(\ln 2 - \frac{5}{8}\right)p_{nm}^2 + \frac{3}{4}\theta_{\text{co}}\left(\frac{r_n}{r_i}\right)^\alpha p_{ij}p_{nm}\right.$$

$$\left. - \frac{\theta_{\text{co}}^2}{8}\left(\frac{r_n}{r_i}\right)^{2\alpha}p_{ij}^2\right) + \sum_{i\in\mathcal{N}_{m-n}}\left(\ln 2 - \frac{5}{8}\right)p_{nm}^2$$

$$+ \frac{3}{4}\theta_{\text{co}}\left(\frac{r_n}{r_i}\right)^\alpha p_{im}p_{nm} - \frac{\theta_{\text{co}}^2}{8}\left(\frac{r_n}{r_i}\right)^{2\alpha}p_{im}^2 \le 0 \tag{36}$$

From (35) and (36), problem (27) can be expressed as

$$\text{Find } \mathbf{p} \tag{37}$$

$$\text{s.t } \text{C1: } 0 \le p_{nm} \le P_{\max} \tag{37a}$$

$$\text{C6: } \ln\left(\frac{\eta}{R_m}\right)p_{nm}^2 + \frac{\tilde{\theta}_m\sigma_c^2 r_n^\alpha}{A(f_c)}p_{nm}$$

$$+ \sum_{j\in\mathcal{M}_{-m}}\sum_{i\in\mathcal{N}_{j-n}}\tilde{\theta}_m\left(\frac{r_n}{r_i}\right)^\alpha p_{ij}p_{nm}$$

$$- \frac{1}{2}\tilde{\theta}_m^2\left(\frac{r_n}{r_i}\right)^{2\alpha}p_{ij}^2 \le 0, \quad \text{if } \sum_{k\in\mathcal{N}_m}s_{km}^* = 1 \tag{37b}$$

$$\text{C7: } \ln\left(\frac{\eta}{R_m}\right)p_{nm}^2 + \frac{\theta_{\text{co}}\sigma_c^2 r_n^\alpha}{A(f_c)}p_{nm}$$

$$+ \left(\sum_{j\in\mathcal{M}_{-m}}\sum_{i\in\mathcal{N}_{j-n}}\left(\ln 2 - \frac{5}{8}\right)p_{nm}^2\right.$$

$$+ \frac{3}{4}\theta_{\text{co}}\left(\frac{r_n}{r_i}\right)^\alpha p_{ij}p_{nm} - \frac{\theta_{\text{co}}^2}{8}\left(\frac{r_n}{r_i}\right)^{2\alpha}p_{ij}^2\right)$$

$$+ \sum_{i\in\mathcal{N}_{m-n}}\left(\ln 2 - \frac{5}{8}\right)p_{nm}^2 + \frac{3}{4}\theta_{\text{co}}\left(\frac{r_n}{r_i}\right)^\alpha p_{im}p_{nm}$$

$$- \frac{\theta_{\text{co}}^2}{8}\left(\frac{r_n}{r_i}\right)^{2\alpha}p_{im}^2 \le 0, \quad \text{if } \sum_{k\in\mathcal{N}_m}s_{km}^* \ge 2 \tag{37c}$$

Problem (37) is a feasibility problem with quadratic inequality constraints. Hence, solutions can be computed by means of solvers such *fmincon* in Matlab.

VII. NUMERICAL RESULTS

A. Simulation Settings

We basically use the simulation parameters of references [11], [20]. Namely, we consider a cell of radius $R = 1$ km, where end-devices are uniformly distributed over the cell, and their locations are fixed during each beacon period but randomly set at each new period. Channels undergo block Rayleigh fading, i.e., small-scale fading channel coefficients are randomly drawn every scheduling period. All results are averaged over 100 sets of position realizations (beacon periods) and 1000 random channel realizations. A duty cycle of 10% is considered firstly, where $50 \sim 200$ end-devices transmit, and finally, a duty cycle of 1% is considered for $500 \sim 2000$ end-devices, giving rise to a very dense environment under challenging interference levels. All devices always have packets to transmit (full buffer assumption) and transmit in a single channel of carrier frequency $f_c = 868$

MHz with a bandwidth $BW = 125$ kHz. We consider a lossy urban environment, with a path loss exponent equal to 4. The maximal transmit power is fixed to $P_{\max} = 14$ dBm. The number of iterations N_I was fixed to 1, as it gives the best compromise between performance and computational complexity. The computer simulation environment has been implemented in Matlab version 9.2. Finally, the throughput results are computed without accounting for MAC overheads for both proposed and reference algorithms.[3]

B. Baseline Schemes

We consider two baseline schemes for performance comparison: the random SF allocation [11], and the distance-SF allocation algorithms [23], with a maximal number of simultaneously transmitting devices equal to $A = \sum_{m \in \mathcal{M}} \mathrm{N}_{\max}(m)$ per scheduling period, for fair comparison with the proposed scheme. The transmit power of all end-devices is set equal to $P_{\max} = 14$ [dBm], since no power allocation schemes had been proposed to jointly tackle co-SF and inter-SF interferences so far.

- **Random SF-allocation (*Conv. Random*)**: at each scheduling period, the gateway chooses randomly A devices among $\mathcal{N}$ and assigns a random SF to each of these devices among the SFs they can successfully receive. The allocated devices are removed from the pool of candidate devices for the next scheduling periods (duty cycle limitation), until the next beacon period.

- **Distance SF-Allocation (*Conv. Distance*)**: at each scheduling period, the gateway chooses randomly A devices among $\mathcal{N}$. Then, the SF for each of these devices is determined by Table I based on their distance r_n: device n uses SF m if $r_n \in (l_{m-1}, l_m]$. As in *Conv. Random*, to comply with the duty cycle limitation, allocated devices are removed from the pool of candidate devices for the next scheduling periods until the next beacon period.

C. Choice of N_{max} Given a Target Minimum Throughput

To determine the quota of each SF, we fix a target minimal throughput equal to 1 bit/s for a given scheduling period (i.e., without duty cycle effects). We have run preliminary simulations over 100000 scheduling frames. Table II represents the minimal short-term average rate achieved on each SF, for different values of $\mathrm{N}_{\max}$. Only co-SF interferences were considered as the goal is to fix the upper-bound on the number of allowed devices per SF. We can observe that to guarantee the target minimal throughput of 1 bit/s, we can have at most three devices assigned to SF 7 but only one device to the other SFs. In the sequel, we consider two scenarios: firstly, where there is no co-SF interferences, i.e., $\mathrm{N}_{\max}(m) = 1 \ \forall m$, and secondly, where both co-SF and inter-SF interferences are present, with at most three end-devices assigned to SF 7 ($\mathrm{N}_{\max}(7) = 3$) and one to the others ($\mathrm{N}_{\max}(m) = 1 \ \forall m \neq 7$). For fair comparison, the number of simultaneously transmitting end-devices A is equal to $\sum_{m \in \mathcal{M}} \mathrm{N}_{\max}(m)$ in each scheduling period.

---

[3]If a realistic MAC layer were implemented, a drop of performance would occur in all algorithms, due to the overhead of the MAC layer.

TABLE II
MINIMAL THROUGHPUT FOR EACH SF m (IN kbits/s)

$\mathrm{N}_{\max}$	SF7	SF8	SF9	SF10	SF11	SF12
1	4.82	1.51	1.06	4.7e-1	2.7e-1	1.9e-1
2	7.7e-2	1.1e-7	9.3e-14	7.8e-25	6.7e-46	3.7e-78
3	2.7e-3	8.2e-9	2e-15	8.2e-27	3.1e-49	1.3e-84
4	9.9e-5	5.8e-10	9.0e-17	4.3e-29	1.2e-49	1.1e-86
5	1.8e-6	5.2e-11	6.5e-18	1.3e-30	1.0e-53	3.7e-93

Note that, given the considered network parameters, i.e., one channel and the two cases of $\mathrm{N}_{\max}$, the proposed method will produce at most eight simultaneous packets to be decoded per scheduling period. This requires eight demodulators at the gateway, which is compatible with current gateways using the Semtech SX1301 chip [24]. Decoding more packets (using more SFs or channels) is possible by increasing the hardware cost at the gateway, or by Software-Defined-Radio (SDR) implementation. In the sequel, proposed and benchmark algorithms are evaluated on a fair basis by assuming the same number of demodulators (eight) on the considered channel.
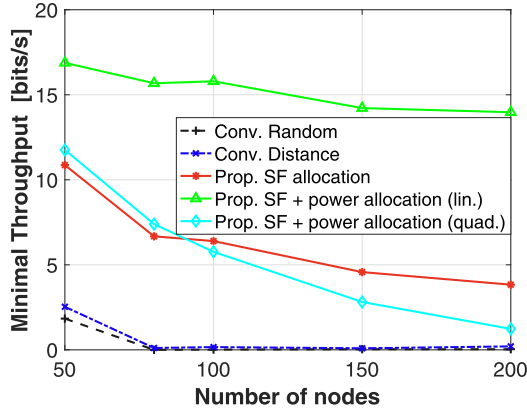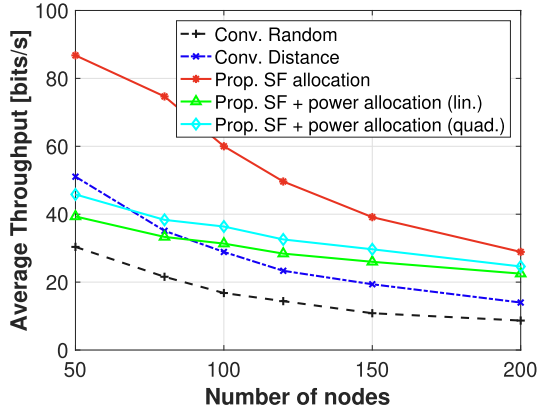
D. Performance Evaluation for $N_{max}(m) = 1, \forall m \in \mathcal{M}$

First let us discuss the case with SF allocation optimization only with maximum transmit power as in baseline schemes, namely the performance of *Prop. SF allocation* (Algorithms 2 and 3). Figure 2 shows the performance comparison of our proposed algorithms, with and without the power optimization step, and the baseline schemes in terms of minimal end-device throughput where the minimum is taken over the allocated devices' short-term average rates in each scheduling period, as a function of a varying number of end-devices. We observe that our proposed *SF allocation* algorithm yields significant performance gains compared to both *Conv. Random* and *Conv. Distance* for all values of N. For instance, Fig. 2 shows that, while baseline schemes lead to an early drop of minimal rate (almost null for $N > 80$), the proposed *SF-allocation* provides a good minimal throughput for a much higher number of end-devices.

Figure 3 shows the performance comparison in terms of average end-device throughput between the different allocation schemes, against a varying number of end-devices. We can clearly see that the proposed *SF allocation* algorithm is superior to all other schemes. From Figure 3, the proposed method can provide an average throughput always larger than 30 bit/s while *Conv. Random* and *Conv. Distance* offer less than half for $N \geq 80$.
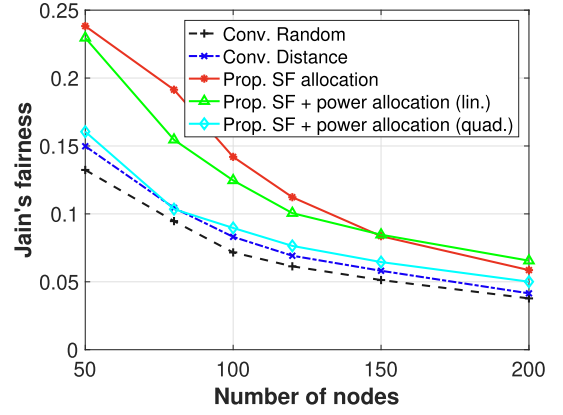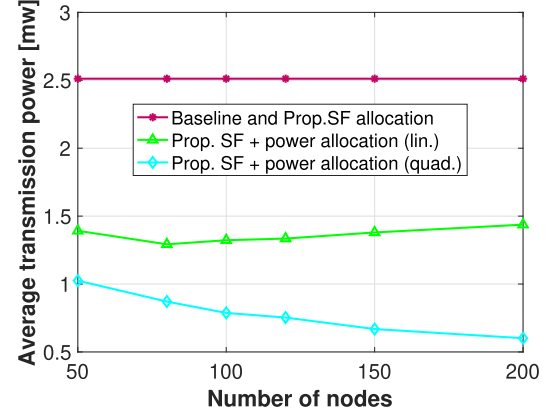
We now evaluate the fairness levels of the different algorithms by using the Jain's fairness index, given by $\mathcal{J} = \dfrac{\left(\sum_{n \in \mathcal{N}} U_n \right)^2}{N \times \sum_{n \in \mathcal{N}} U_n^2}$. Figure 4 shows that by the considered max-min strategy and matching-based methodology, proposed *SF allocation* improves well the system fairness level compared to baseline methods.

Next, we discuss the performance of the proposed joint SF and power allocation algorithms, shown in Figs. 2, 3, and 4. Firstly, we observe that the proposed power allocation methods

Fig. 2.   Minimal end-device throughput, $\mathrm{N}_{\max}(7) = 1$.

Fig. 4.   Jain's fairness metric, $\mathrm{N}_{\max}(7) = 1$.

Fig. 3.   Average end-device throughput, $\mathrm{N}_{\max}(7) = 1$.

Fig. 5.   Average power consumption, $\mathrm{N}_{\max}(7) = 1$.

in Algorithm 4, with linear and quadratic approximations, outperform both baseline schemes in terms of minimal end-device throughputs. However, when N is larger than 100, we can observe a decrease in the minimal throughput of the quadratic approximation compared to our proposed SF-allocation algorithm. This is due to the use of the quadratic approximation which does not necessarily guarantee a better local optimum compared to that offered by linear approximation, as this depends on the difference between the solution sets of the approximated problems - linear and quadratic cases-, and that of the original problem, given its non-linearity. Hence, there are no theoretical guarantees that quadratic approximation should be superior to linear approximation, nor that it should outperform the fixed power allocation case of the original problem. However, both approximations yield much higher minimal throughputs compared to baseline schemes. Along with higher minimal throughput, Fig. 4 shows the large fairness improvements brought by our joint SF and power allocation with linear approximation, against baseline while achieving higher average throughput for $N \geq 80$, as shown in Fig 3.

Finally, Fig. 5 depicts the average transmit power consumed by end-devices with a varying number of nodes. We can observe that the proposed joint allocation schemes enable important savings in energy consumption while providing better throughput and higher fairness compared to the fixed transmit power allocation approaches. We also notice that with a quadratic approximation, Algorithm 4 allows even

higher power savings, i.e., up to 58%, jointly with a higher average throughput, compared to the linear approximation case. That is, in the linear case, more power is spent for low channel quality users in order to maintain high minimal average rates. On the contrary, solutions obtained by quadratic approximation tend to decrease power consumption, at the expense of lower minimal throughputs as shown in Fig. 2. These observations suggest that with quadratic approximation, the global interference level is limited compared to the linear case, but at the detriment of useful signal power of the end-devices with lower channel qualities.

E. Performance Evaluation for $N_{max}(m) = 3$ for $m = 7$, $N_{max}(m) = 1$ for $m \neq 7$

For the second scenario, Fig. 6 depicts the performance comparison of our proposed algorithms with and without joint power allocation optimization step, and the baseline schemes. From Fig. 6 we can first confirm that *Prop. SF allocation* algorithm still largely outperforms baseline schemes even when increasing $\mathrm{N}_{\max}(7)$. However, its performance decreases compared to the case of Fig. 2 where there are no co-SF interferences.

Fig. 7 shows the impact of maximizing the minimal short-term average rates on the average end-device throughput. This time, the gain in minimal throughput comes at the cost of a poorer average throughput compared to baselines, as maintaining a high minimal throughput is very challenging whenever there are both inter-SF and co-SF interferences. Note
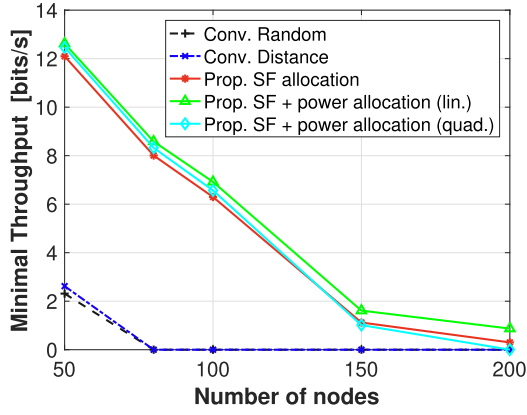
Fig. 6.   Minimal end-device throughput, $N_{max}(7) = 3$.
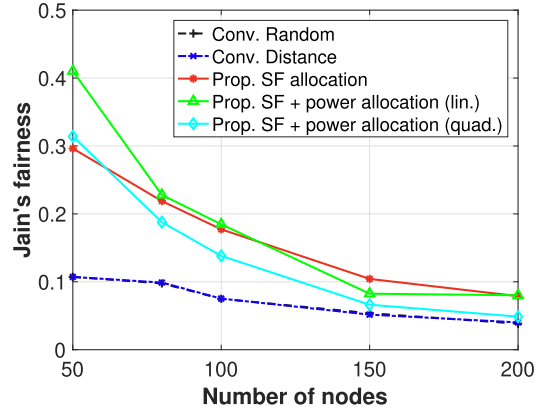
Fig. 8.   Jain's fairness metric, $N_{max}(7) = 3$.
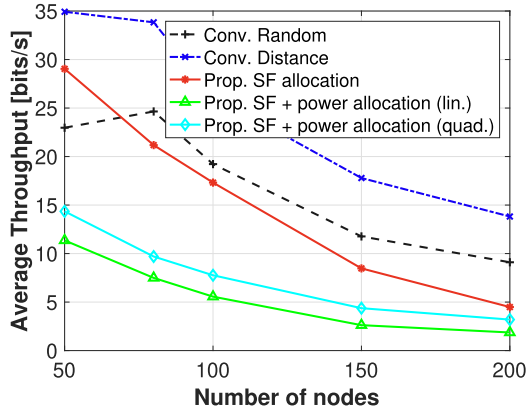
Fig. 7.   Average end-device throughput, $N_{max}(7) = 3$.
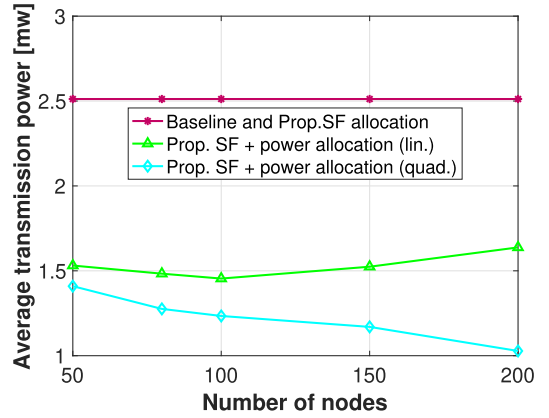
Fig. 9.   Average power consumption, $N_{max}(7) = 3$.

that the proposed solution with quadratic approximation offers a slightly higher average throughput compared to the linear case.

From Figure 8, it is clear that the proposed approaches bring significant performance gains in terms of fairness, which is in line with the minimal throughput gains. In addition, the proposed power optimization still enables high fairness improvements, even under both inter-SF and co-SF interferences, with a larger gain for the linear approximation. It is hence worthwhile noting that, by allowing co-SF interferences with $N_{max}(7) = 3$, the general fairness level is notably increased compared to the case of $N_{max}(7) = 1$ in Fig. 4.

Finally, Fig. 9 shows the drastic energy savings offered by our proposed power optimization (up to 60%), compared to baseline and proposed SF-allocation only. Similarly to scenario 1, the quadratic approximation offers further power savings jointly with a higher average throughput, compared to linear approximation. We also note that with $N_{max}(7) = 3$, more power is consumed in both linear and quadratic approximation cases as compared to $N_{max}(7) = 1$, since more end-devices are allocated SFs.

Overall, the proposed joint SF assignment and power allocation method provides remarkable performance improvements, jointly in terms of minimal achievable rates, average throughput, fairness, and consumed energy. These joint improvements come at the price of higher computational complexity at the

network server, and may thus require higher computation time. Hence, the proposed method is applicable to scenarios where end-devices are static or with low-mobility.

F. SF-Allocation Distribution

In this subsection, we compare the distribution of the number of end-devices allocated to each SF for proposed and benchmark algorithms in the case $N = 200$.

Figures 10(a) and 10(b) show that *Conv. Random* tends to allocate more end-devices to SF 12 compared to SF 7. Indeed, only the end-devices that are close to the sink can obtain SF 7, while all end-devices can obtain SF 12. In *Conv. Distance*, the SFs are assigned according to the distance of the end-devices to the gateway. For an end-device n, the probability of selecting SF m is then given by $q_m = \int_{l_{m-1}}^{l_m} \frac{2r_n}{R^2} dr_n$ [11], whose values are given by $q_7 = 0.21$, $q_8 = 0.08$, $q_9 = 0.12$, $q_{10} = 0.17$, $q_{11} = 0.19$, $q_{12} = 0.23$ resulting into the proportions of Fig. 10. The main issue with this strategy is that end-devices located in the same annulus will be assigned to the same SF, even if there are other available SFs that they can use, thereby increasing co-SF interferences. For $N_{max}(7) = 3$, *Prop. SF allocation* clearly allocates a larger proportion of SF 7 with larger achievable rates, hence reducing the allocation of higher SFs with lower achievable rates. This is enabled by optimizing the allocation of SF 7, the most vulnerable
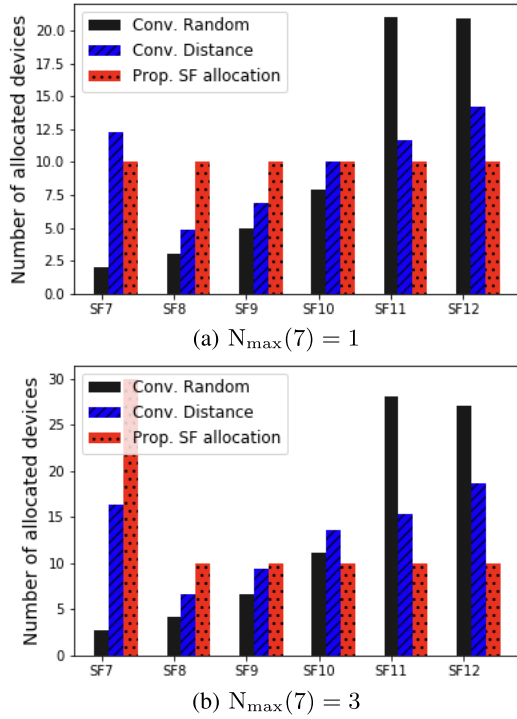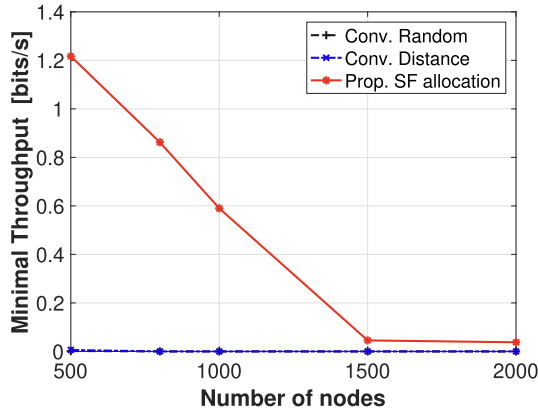
(a) $N_{max}(7) = 1$

(b) $N_{max}(7) = 3$

Fig. 10. Distribution of number of allocated devices per SF.

Fig. 11. Minimal end-device throughput, $N_{max}(7) = 3$ and $dc = 1\%$.

Fig. 12. Average end-device throughput, $N_{max}(7) = 3$ and $dc = 1\%$.

Fig. 13. Jain's fairness metric, $N_{max}(7) = 3$ and $dc = 1\%$.

Fig. 14. Distribution of number of allocated devices per SF.

albeit most spectrum-efficient SF, by opportunistically taking advantage of the large-scale random channel fluctuations while being aware of both co-SF and inter-SF interferences. Our proposed methods thus enable an opportunistic SF allocation that jointly enhances minimum device rates, average rates and device fairness.

G. Duty Cycle Equal to 1%, $N_{max}(m) = 3$ for $m = 7$, $N_{max}(m) = 1$ for $m \neq 7$

Finally, we evaluate the proposed SF allocation algorithm and benchmark schemes under a duty cycle of 1%. Figures 11, 12 and 13 show the performances of minimal throughput, average throughput and Jain's fairness for $500 \sim 2000$ end-devices, respectively, while Fig. 14 illustrates the distribution of the number of allocated devices over SFs in the case of 2000 devices.
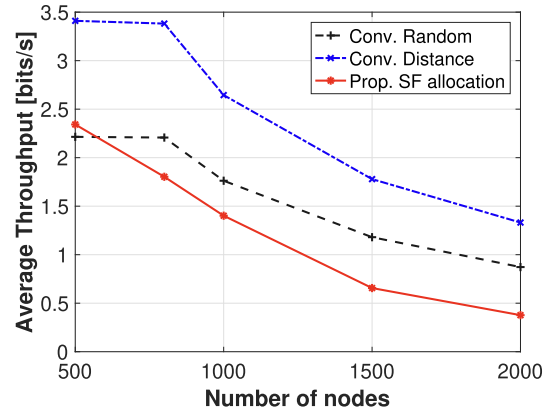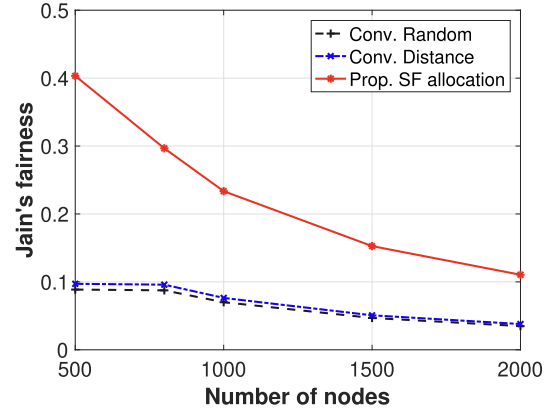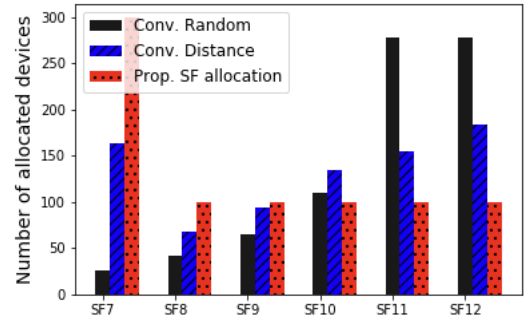
We can observe that, while the minimal throughputs achieved by benchmark schemes are almost null in such dense networks, *Prop. SF allocation* enables much higher minimal throughput and fairness levels even for 2000 devices, at the cost of lower average throughput. This illustrates that the proposed method scales well in terms of minimal throughput and fairness, which are particularly challenging in dense networks.

VIII. CONCLUSION

In this work, we have addressed the issue of network performance enhancement for a LPWAN based on LoRa physical layer, where both impacts of co-SF and inter-SF interferences were included. Focusing on user fairness improvement for

uplink communications, the objective was to optimize SFs' assignment and transmit power allocation for maximizing the minimal short-term average user rates, whose expressions are in line with the LoRa system requirements by not assuming instantaneous CSIs. The intractability of the joint SF and power allocation problem is tackled by separating it into two subproblems: SF assignment under fixed power, and power allocation under fixed SFs. Simulation results show that, despite severe co-SF and inter-SF interferences, our proposed algorithms outperformed baseline algorithms, jointly in terms of minimal device rates, user fairness, and average device throughput. Both proposed linear and quadratic approximation approaches to the non-linear feasibility problem for power allocation were shown to provide efficient transmit power solutions, leading to drastic energy savings, while further enhancing minimal throughput and user fairness. In the future work, the proposed methods will be extended for multi-cell LoRa systems by assigning end-devices to the best gateway for downlink messages in the case of multiple gateways, as well as for more sophisticated application scenarios including heterogeneous environments and high device mobility.

APPENDIX

A. Proposed SF-Allocation Algorithm Analysis Proofs

Proposition 1 (Stability): When the proposed algorithm terminates, it finds a two-sided exchange stable matching.

Proof: Let us assume that the proposed SF-allocation algorithm terminates and the final matching is not two-sided exchange stable. Then, the matching contains at least one more blocking pair (k, m) or (n, l) where the utility of at least one player among $\{n, m, k, l\}$, can be improved without lowering the others' utility. Accordingly, the proposed algorithm would continue, thereby the matching would not be final, which contradicts the initial assumption. □

Proposition 2 (Convergence): After a finite number of swap operations, the algorithm eventually converges to a two-sided exchange stable matching.

Proof: A swap operation occurs if it improves the utility of at least one player without decreasing the others', hence the utilities can only rise. Additionally, the maximal throughput that can be achieved on an SF m is upper-bounded by the data bit-rate R_m, meaning that each SF m and the end-devices assigned to it have utilities upper bounded by R_m.

The number of potential swap operations is finite: end-device assigned to SF l can make at most $\mathrm{N_{max}}(l) \times \sum_{j \in \mathcal{M}_{-l}} \mathrm{N_{max}}(j)$ swap operations. The total number of swap operations is thus upper-bounded by $\sum_{l \in \mathcal{M}} \mathrm{N_{max}}(l) \times \sum_{j \in \mathcal{M}_{-l}} \mathrm{N_{max}}(j)$. □

Proposition 3 (Complexity): The running time of our proposed algorithm is upper-bounded by $\mathcal{O}(NM + Q^2 M^2)$, where $Q = \max_{m \in \mathcal{M}}\{\mathrm{N_{max}}(m)\}$.

Proof: Initial matching complexity: in the worst case, all the end-devices have the same preference list, and they are located in the area covered by all the SFs. At round$_1$ the gateway receives N requests, at round$_2$ it receives $N - \mathrm{N_{max}}(m_1)$

requests, at round$_i$ it receives $N - \sum_{k=1}^{i-1} \mathrm{N_{max}}(m_k)$ requests. Therefore, the total number of requests equals $NM - \sum_{i=1}^{M-1}(M - i) \times \mathrm{N_{max}}(m_i)$. The complexity of the initial matching is upper bounded by: $\mathcal{O}(NM)$.

Matching refinement complexity: in each iteration, for each SF m, the algorithm considers at most $\mathrm{N_{max}}(m)$ end-devices and examines $\sum_{l \in \mathcal{M}_{-m}} \mathrm{N_{max}}(l)$ swap operations for each of these end-devices. Therefore, the number of swap operations that are examined in one iteration is upper bounded by $\sum_{m \in \mathcal{M}} \mathrm{N_{max}}(m) \times \sum_{l \in \mathcal{M}_{-m}} \mathrm{N_{max}}(l)$. Let $Q = \max_{m \in \mathcal{M}}\{\mathrm{N_{max}}(m)\}$, thus the computational complexity of the matching refinement is upper bounded by $\mathcal{O}(Q^2 M(M-1))$.

In summary, the computational complexity of our algorithm is upper bounded by $\mathcal{O}\left(NM + Q^2 M^2\right)$. □

B. Linear Approximation of Power Allocation Optimization

1) Case 1: The term $\tilde{\theta}_m \frac{p_{ij}}{p_{nm}}\left(\frac{r_n}{r_i}\right)^{\alpha}$ in the logarithm of (29) is dominated by the inter-SF interference capture threshold $\tilde{\theta}_m$, which takes very small values as can be observed from Table I. Thus, the term $\tilde{\theta}_m \frac{p_{ij}}{p_{nm}}\left(\frac{r_n}{r_i}\right)^{\alpha}$ will be generally close to zero, as confirmed by the numerical evaluations in Section VII. Therefore, we can approximate the logarithmic term using the Taylor-Maclaurin series,

$$\ln\left(\tilde{\theta}_m \frac{p_{ij}}{p_{nm}}\left(\frac{r_n}{r_i}\right)^{\alpha} + 1\right) = \tilde{\theta}_m \frac{p_{ij}}{p_{nm}}\left(\frac{r_n}{r_i}\right)^{\alpha}$$
$$+ o\left(\tilde{\theta}_m \frac{p_{ij}}{p_{nm}}\left(\frac{r_n}{r_i}\right)^{\alpha}\right), \quad (38)$$

where $o\left(\tilde{\theta}_m \frac{p_{ij}}{p_{nm}}\left(\frac{r_n}{r_i}\right)^{\alpha}\right)$ denotes the remainder of the Taylor series.

By substituting $\ln\left(\tilde{\theta}_m \frac{p_{ij}}{p_{nm}}\left(\frac{r_n}{r_i}\right)^{\alpha} + 1\right)$ by its approximation (38) in (29) and rearranging, we get the following linear inequalities,

$$\ln\left(\frac{\eta}{R_m}\right) p_{nm} + \sum_{j \in \mathcal{M}_{-m}} \sum_{i \in \mathcal{N}_{j-n}} \tilde{\theta}_m \left(\frac{r_n}{r_i}\right)^{\alpha} p_{ij}$$
$$\leq -\frac{\tilde{\theta}_m \sigma_c^2 r_n^{\alpha}}{\mathrm{A}(f_c)}, \quad \forall m \in \mathcal{M}. \quad (39)$$

2) Case 2: Similarly to Case 1, we perform the following linearization in order to make problem (27) tractable. By rearranging the inequalities, we obtain for all $m \in \mathcal{M}$,

$$-\frac{\theta_{\mathrm{co}} \sigma_c^2 r_n^{\alpha}}{A(f_c) p_{nm}} - \sum_{j \in \mathcal{M}_{-m}} \sum_{i \in \mathcal{N}_{j-n}} \ln\left(\theta_{\mathrm{co}} \frac{p_{ij}}{p_{nm}}\left(\frac{r_n}{r_i}\right)^{\alpha} + 1\right)$$
$$- \sum_{i \in \mathcal{N}_{m-n}} \ln\left(\theta_{\mathrm{co}} \frac{p_{im}}{p_{nm}}\left(\frac{r_n}{r_i}\right)^{\alpha} + 1\right) \geq \ln\left(\frac{\eta}{R_m}\right). \quad (40)$$

However, in this case, the co-SF interference capture threshold θ_{co} no longer induces small values of $\theta_{\mathrm{co}} \frac{p_{im}}{p_{nm}}\left(\frac{r_n}{r_i}\right)^{\alpha}$, since in practice, $\theta_{\mathrm{co}} = 6$ dB [20]. Therefore, we now make use of a different approximation based on Taylor's theorem.

Let $g(x) = \ln\left(\frac{\theta_{\text{co}}}{p_{nm}}\left(\frac{r_n}{r_i}\right)^\alpha x + 1\right)$. Clearly, g is a twice continuously differentiable function. From Taylor's theorem, we have

$$g(x) = g(a) + g'(a)(x-a) + \text{o}(x-a), \quad \forall a \in \mathbb{R}^+. \quad (41)$$

Taking $a = \left(\frac{r_i}{r_n}\right)^\alpha \frac{p_{nm}}{\theta_{\text{co}}}$ and given

$$g'(x) = \frac{\frac{\theta_{\text{co}}}{p_{nm}}\left(\frac{r_i}{r_i}\right)^\alpha}{\frac{\theta_{\text{co}}}{p_{nm}}\left(\frac{r_n}{r_i}\right)^\alpha x + 1} = \frac{1}{x+a}, \quad (42)$$

(41) may be written

$$g(x) = \left(\ln(2) - \frac{1}{2}\right) + \frac{\theta_{\text{co}}}{2p_{nm}}\left(\frac{r_n}{r_i}\right)^\alpha x$$
$$+ \text{o}\left(x - \left(\frac{r_i}{r_n}\right)^\alpha \frac{p_{nm}}{\theta_{co}}\right). \quad (43)$$

Dropping the remainder o and substituting the logarithmic terms of (40) by their linear expressions in (43) and taking $x = p_{ij}$, we obtain the linearized expressions

$$\frac{\theta_{\text{co}}\sigma_c^2 r_n^\alpha}{A(f_c)p_{nm}} + \left(\sum_{j\in\mathcal{M}_{-m}}\sum_{i\in\mathcal{N}_{j-n}} \ln(2) - \frac{1}{2} + \frac{\theta_{\text{co}}}{2}\left(\frac{r_n}{r_i}\right)^\alpha \frac{p_{ij}}{p_{nm}}\right)$$
$$+ \sum_{i\in\mathcal{N}_{m-n}} \ln(2) - \frac{1}{2} + \frac{\theta_{\text{co}}}{2}\left(\frac{r_n}{r_i}\right)^\alpha \frac{p_{im}}{p_{nm}} \leq -\ln\left(\frac{\eta}{R_m}\right). \quad (44)$$

C. Quadratic Approximation of Power Allocation Optimization

let $g(x) = \ln\left(\theta_{\text{co}}\frac{x}{p_{nm}}\left(\frac{r_n}{r_i}\right)^\alpha + 1\right)$. g is a twice continuously differentiable function. From Taylor's theorem, we have,

$$g(x) = g(a) + g'(a)(x-a) + \frac{g''(a)}{2!}(x-a)^2$$
$$+ \text{o}\left((x-a)^2\right), \quad \forall a \in \mathbb{R}^+. \quad (45)$$

The first derivative of g is given in (42), and its second derivative by

$$g''(x) = -\frac{\frac{\theta_{\text{co}}^2}{p_{nm}^2}\left(\frac{r_n}{r_i}\right)^{2\alpha}}{\left(\theta_{\text{co}}\frac{x}{p_{nm}}\left(\frac{r_n}{r_i}\right)^\alpha + 1\right)^2} = \frac{-1}{(x+a)^2}. \quad (46)$$

From (45), the quadratic approximation of g centered at $a = \left(\frac{r_i}{r_n}\right)^\alpha \frac{p_{nm}}{\theta_{\text{co}}}$ and for $x = p_{ij}$, is given by,

$$g(p_{ij})$$
$$= \left(\ln 2 - \frac{5}{8}\right) + \frac{3}{4}\theta_{\text{co}}\left(\frac{r_n}{r_i}\right)^\alpha \frac{p_{ij}}{p_{nm}}$$
$$- \frac{\theta_{\text{co}}^2}{8}\left(\frac{r_n}{r_i}\right)^{2\alpha}\frac{p_{ij}^2}{p_{nm}^2} + \text{o}\left(\left(p_{ij} - \left(\frac{r_i}{r_n}\right)^\alpha\frac{p_{nm}}{\theta_{\text{co}}}\right)^2\right), \quad (47)$$

and for $x = p_{im}$,

$$g(p_{im})$$

$$= \left(\ln 2 - \frac{5}{8}\right) + \frac{3}{4}\theta_{\text{co}}\left(\frac{r_n}{r_i}\right)^\alpha \frac{p_{im}}{p_{nm}}$$
$$- \frac{\theta_{\text{co}}^2}{8}\left(\frac{r_n}{r_i}\right)^{2\alpha}\frac{p_{im}^2}{p_{nm}^2} + \text{o}\left(\left(p_{im} - \left(\frac{r_i}{r_n}\right)^\alpha\frac{p_{nm}}{\theta_{\text{co}}}\right)^2\right). \quad (48)$$

Finally by dropping the remainder (40) becomes,

$$\frac{\theta_{\text{co}}\sigma_c^2 r_n^\alpha}{A(f_c)p_{nm}} + \left(\sum_{j\in\mathcal{M}_{-m}}\sum_{i\in\mathcal{N}_{j-n}}\left(\ln 2 - \frac{5}{8}\right)\right.$$
$$+ \frac{3}{4}\theta_{\text{co}}\left(\frac{r_n}{r_i}\right)^\alpha \frac{p_{ij}}{p_{nm}} - \frac{\theta_{\text{co}}^2}{8}\left(\frac{r_n}{r_i}\right)^{2\alpha}\frac{p_{ij}^2}{p_{nm}^2}\right)$$
$$+ \sum_{i\in\mathcal{N}_{m-n}}\left(\ln 2 - \frac{5}{8}\right) + \frac{3}{4}\theta_{\text{co}}\left(\frac{r_n}{r_i}\right)^\alpha \frac{p_{im}}{p_{nm}}$$
$$- \frac{\theta_{\text{co}}^2}{8}\left(\frac{r_n}{r_i}\right)^{2\alpha}\frac{p_{im}^2}{p_{nm}^2}$$
$$\leq -\ln\left(\frac{\eta}{R_m}\right). \quad (49)$$

By multiplying both sides by p_{nm}^2 we obtain,

$$\ln\left(\frac{\eta}{R_m}\right)p_{nm}^2 + \frac{\theta_{\text{co}}\sigma_c^2 r_n^\alpha}{A(f_c)}p_{nm}$$
$$+ \left(\sum_{j\in\mathcal{M}_{-m}}\sum_{i\in\mathcal{N}_{j-n}}\left(\ln 2 - \frac{5}{8}\right)p_{nm}^2 + \frac{3}{4}\theta_{\text{co}}\left(\frac{r_n}{r_i}\right)^\alpha p_{ij}p_{nm}\right.$$
$$- \frac{\theta_{\text{co}}^2}{8}\left(\frac{r_n}{r_i}\right)^{2\alpha}p_{ij}^2\right) + \sum_{i\in\mathcal{N}_{m-n}}\left(\ln 2 - \frac{5}{8}\right)p_{nm}^2$$
$$+ \frac{3}{4}\theta_{\text{co}}\left(\frac{r_n}{r_i}\right)^\alpha p_{im}p_{nm} - \frac{\theta_{\text{co}}^2}{8}\left(\frac{r_n}{r_i}\right)^{2\alpha}p_{im}^2 \leq 0 \quad (50)$$

REFERENCES

[1] L. Amichi, M. Kaneko, N. E. Rachkidy, and A. Guitton, "Spreading factor allocation strategy for LoRa networks under imperfect orthogonality," in *Proc. IEEE Int. Conf. Commun. (ICC)*, May 2019, pp. 1–7.

[2] *Sigfox*. Accessed: Feb. 26, 2020. [Online]. Available: http://www.sigfox.com

[3] *Ingenu*. Accessed: Feb. 26, 2020. [Online]. Available: http://www.ingenu.com

[4] LoRa Alliance. *LoRaWAN-What is it? A Technical Overview of LoRa and LoRaWAN?*. Accessed: Apr. 21, 2019. [Online]. Available: http://www.lora-alliance.org

[5] J. Haxhibeqiri, F. Van den Abeele, I. Moerman, and J. Hoebeke, "LoRa scalability: A simulation model based on interference measurements," in *Sensors*, vol. 17, no. 6, p. 1193, May 2017.

[6] Semtech Corporation. (2013). *LoRa Modem Design Guide, SX1272/3/6/7/8*. Accessed: Apr. 21, 2019. [Online]. Available: http://www.semtech.com

[7] LoRa Alliance. *LoRa Alliance LoRaWAN 1.1 Specification*. Accessed: Feb. 26, 2020. [Online]. Available: https://lora-alliance.org/sites/default/files/2018-04/lorawantm_specification_-v1.1.pdf

[8] D. Croce, M. Gucciardo, I. Tinnirello, D. Garlisi, and S. Mangione, "Impact of spreading factor imperfect orthogonality in LoRa communications," in *Towards a Smart and Secure Future Internet*, vol. 766. Cham, Switzerland: Springer, 2017, pp. 6510–6523.

[9] G. Zhu, C.-H. Liao, M. Suzuki, Y. Narusue, and H. Morikawa, "Evaluation of LoRa receiver performance under co-technology interference," in *Proc. 15th IEEE Annu. Consum. Commun. Netw. Conf. (CCNC)*, Jan. 2018.

[10] A. Mahmood, E. Sisinni, L. Guntupalli, R. Rondon, S. A. Hassan, and M. Gidlund, "Scalability analysis of a LoRa network under imperfect orthogonality," *IEEE Trans Ind. Informat.*, vol. 15, no. 3, pp. 1425–1436, Mar. 2019.

[11] A. Waret, M. Kaneko, A. Guitton, and N. El Rachkidy, "LoRa through-put analysis with imperfect spreading factor orthogonality," *IEEE Wireless Commun. Lett.*, vol. 8, no. 2, pp. 408–411, Apr. 2019.

[12] Z. Qin and J. A. McCann, "Resource efficiency in low-power wide-area networks for IoT applications," in *Proc. IEEE Global Commun. Conf. (GLOBECOM)*, Dec. 2017, pp. 1–7.

[13] B. Reynders, W. Meert, and S. Pollin, "Power and spreading factor control in low power wide area networks," in *Proc. IEEE Int. Conf. Commun. (ICC)*, May 2017, pp. 1–5.

[14] N. E. Rachkidy, A. Guitton, and M. Kaneko, "Decoding superposed LoRa signals," in *Proc. IEEE 43rd Conf. Local Comput. Netw. (LCN)*, Chicago, IL, USA, Oct. 2018, pp. 184–190.

[15] I. E. Korbi, Y. Ghamri-Doudane, and L. A. Saidane, "LoRaWAN analysis under unsaturated traffic, orthogonal and non-orthogonal spreading factor conditions," in *Proc. IEEE 17th Int. Symp. Netw. Comput. Appl. (NCA)*, Nov. 2018.

[16] L. Beltramelli, A. Mahmood, M. Gidlund, P. Österberg, and U. Jennehag, "Interference modelling in a multi-cell LoRa system," in *Proc. 14th Int. Conf. Wireless Mobile Comput., Netw. Commun. (WiMob)*, Oct. 2018, pp. 1–8.

[17] N. El Rachkidy, A. Guitton, and M. Kaneko, "Collision resolution protocol for delay and energy efficient LoRa networks," *IEEE Trans. Green Commun. Netw.*, vol. 3, no. 2, pp. 535–551, Jun. 2019.

[18] X. Liu, Z. Qin, Y. Gao, and J. A. McCann, "Resource allocation in wireless powered IoT networks," *IEEE Internet Things J.*, vol. 6, no. 3, pp. 4935–4945, Jun. 2019.

[19] A. Augustin, J. Yi, T. Clausen, and W. M. Townsley, "A study of LoRa: Long range & low power networks for the Internet of Things," *Sensors*, vol. 16, no. 9, p. 1466, Sep. 2016.

[20] O. Georgiou and U. Raza, "Low power wide area network analysis: Can LoRa scale?" *IEEE Wireless Commun. Lett.*, vol. 6, no. 2, pp. 162–165, Apr. 2017.

[21] R. Kannan and C. L. Monma, "On the computational complexity of integer programming problems," in *Optimization and Operations Research*. Berlin, Germany: Springer-Verlag, 1978, pp. 161–172.

[22] Y. Gu, W. Saad, M. Bennis, M. Debbah, and Z. Han, "Matching theory for future wireless networks: Fundamentals and applications," *IEEE Commun. Mag.*, vol. 53, no. 5, pp. 52–59, May 2015.

[23] M. Bor, U. Roedig, T. Voigt, and J. M. Alonso, "Do LoRa low-power wide-area networks scale?" in *19th ACM Int. Conf. Modeling, Anal. Simulation Wireless Mobile Syst.*, Nov. 2016, pp. 59–67.

[24] Semtech Corporation. *Digital Baseband Chip for Outdoor LoRaWAN, Macro Gateways*. Accessed: Feb. 26, 2020. [Online]. Available: http://www.semtech.com/products/wireless-rf/lora-gateways/sx1301
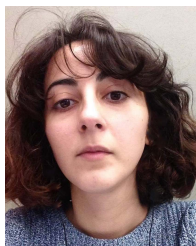
Megumi Kaneko (Senior Member, IEEE) received the Diplôme d'Ingénieur from Télécom SudParis (French Grande Ecole), France, jointly the M.Sc. degree from Aalborg University, Denmark, the Ph.D. degree from Aalborg University in 2007, and the HDR (Habilitation à Diriger des Recherches) degree from Paris-Saclay University, France, in May 2017. She was a JSPS Post-Doctoral Fellow with Kyoto University from April 2008 to August 2010. From September 2010 to March 2016, she was an Assistant Professor with the Department of Systems Science, Graduate School of Informatics, Kyoto University. She is currently an Associate Professor with the National Institute of Informatics and also with the Graduate University for Advanced Studies (Sokendai), Tokyo, Japan. Her research interests include wireless communications, 5G and beyond, IoT wireless systems, and PHY/MAC design and optimization. She received the 2009 Ericsson Young Scientist Award, the IEEE GLOBECOM 2009 Best Paper Award, the 2011 Funai Young Researcher's Award, the WPMC 2011 Best Paper Award, the 2012 Telecom System Technology Award, the 2016 Inamori Foundation Research Grant, and the 2019 Young Scientists' Prize from the Minister of Education, Culture, Sports, Science and Technology of Japan. She serves as an Editor of IEEE TRANSACTIONS ON WIRELESS COMMUNICATIONS, IEEE COMMUNICATION LETTERS, and *IEICE Transactions on Communications*.

Ellen Hidemi Fukuda received the bachelor's and master's degrees in computer science and the Ph.D. degree in applied mathematics from the University of São Paulo, Brazil, in 2011. She is currently an Associate Professor with the Graduate School of Informatics, Kyoto University, Japan. Her research interests include the development of methods for continuous optimization and applications of optimization, including wireless communications.

Nancy El Rachkidy received the Ph.D. degree from Université Blaise Pascal in 2011 and the M.Sc. degree in networks and computer science from the Lebanese University of Beirut, Lebanon, in 2006. She is currently an Assistant Professor with Université Clermont Auvergne, France. She is doing her research at LIMOS—CNRS. Her research interests include wireless communincations, sensor network, MAC and routing protocols.

Licia Amichi received the B.S. degree in computer science from the Pierre and Marie Curie University of Paris, France, in 2016, and the M.S. degree in computer science option smart mobility and Internet of Things from Sorbonne University, France, in 2018. She is currently pursuing the Ph.D. degree with INRIA Saclay and École Polytechnique, France. From February to August 2018, she was an Intern with the National Institute of Informatics, where she worked on IoT wireless networks. Her current research interests include IoT wireless network, mobility modeling and prediction, and datamining.

Alexandre Guitton received the Ph.D. degree in computer networks from the University of Rennes I, France, in 2005, and the HDR (habilitation to lead research activities) degree from Université Blaise Pascal, France, in 2014. He is currently a Full Professor of computer science with Université Clermont Auvergne, France. He is also a Researcher with the LIMOS—CNRS laboratory. His research interests include wireless communications, sensor networks, MAC protocols, routing protocols (including loop detection and removal), and energy-efficiency.